Utilizing recycled waste organic muck and phosphogypsum in controlled low-strength materials: An experimental study on engineering properties and environmental safety

Yue Gui [a], Zhibin Zi [a], Jim Shiau [b], Shisong Yuan [a], Lun Hua [a], Ling Sun [a], Yi Tian [a], Shiqi Li [a], Manlin Liu [a],*

[a] *Department of Civil Engineering, Faculty of Civil Engineering and Mechanics, Kunming University of Science and Technology, Kunming, Yunnan, China*
[b] *School of Engineering, University of Southern Queensland, Toowoomba, QLD, Australia*

ARTICLE INFO

ABSTRACT

This study develops a novel organic muck (OM)-phosphogypsum (PG)-based Controlled Low-Strength Material (OP-CLSM) to enable large-scale reuse of these two wastes. It also systematically evaluates the feasibility of using OM-PG mixtures as fine aggregates for CLSM preparation. In this formulation, OM and PG are combined with Ordinary Portland cement (OPC), fly ash (FA), and various admixtures, including polycarboxylate superplasticizer (PCE), calcium chloride ($CaCl_2$), and triethanolamine (TEA). A total of 18 groups of specimens are prepared with varying mix proportions to investigate the effects of the OM: PG mass mixing ratio (M_{OM}: M_{PG}), the organic matter content (w_u) of OM, the OPC: FA mixing ratio (a_{OPC}: a_{FA}), and the incorporation of different admixtures. Systematic laboratory experiments are conducted to evaluate the fresh-state properties, including flowability, bleeding rate, and setting time, as well as the hardened-state property of unconfined compressive strength (UCS). The mineral composition and microstructural characteristics of OP-CLSM are analyzed using X-ray diffraction (XRD) and scanning electron microscopy (SEM). Furthermore, the environmental safety of OP-CLSM is assessed by measuring its pH and examining the Leachability of potentially hazardous substances. Results indicate that, with appropriate mix proportions, OP-CLSM achieves high flowability (>150 mm), an acceptable bleeding rate (0.7–7.0 %), a short setting time (<24 h), and a moderate UCS (0.3–1.8 MPa). The pH ranges from 10 to 12, and the leached concentrations of potentially hazardous substances comply with regulatory standards. Among the tested admixtures, PCE demonstrates superior performance in enhancing flowability, reducing bleeding rate and setting time, and improving UCS. With an optimized mix design, OP-CLSM exhibits promising mechanical and environmental performance, providing a sustainable solution for the reuse of waste materials.

---

1. Introduction

Peaty soil is formed by the incomplete decomposition and accumulation of plant residues in lakes, low-lying areas, and swamp regions during the Quaternary geological period under oxygen-deficient conditions, with a defining feature of high organic matter content (w_u: 10 %–80 % of dry soil mass, locally up to 98 %) [1]. Globally, it spans 59 countries/regions (over 4.15 million km²) [2], while in China it covers approximately 42,000 km² [3]. Due to the porous structure of organic matter and its strong water-retention capacity, peaty soil generally exhibits high water content, a large void ratio, low shear strength, significant compressibility, and creep characteristics. As a result, it is considered a special type of soil with notably poor engineering properties [4]. When subjected to structural loads, peaty soil foundations are prone to excessive or uneven settlement, potentially leading to instability or structural damage. Consequently, foundation improvement or the adoption of pile foundations is often necessary. Additionally, the excavated organic muck (OM) is unsuitable for engineering fill, as its w_u exceeds the standard limit ($w_u \leq 5$ %) [5].

The chemical stabilization/solidification (S/S) method involves incorporating binding agents, such as cement, lime, and fly ash, into the soil. Cementitious substances are generated through hydration, pozzolanic reactions that bind soil particles, and fill voids [6]. This process enhances the soil's strength, stiffness, and impermeability, thereby effectively mitigating adverse properties such as collapsibility, expansibility, and water sensitivity. As a result, the S/S method enables the reuse of problematic soils (e.g., soft soil, collapsible loess, and expansive soil) and solid waste materials (e.g., phosphogypsum, red mud) that would otherwise be unsuitable for use as engineering fill materials. However, previous studies have shown that excessive organic matter can significantly inhibit the solidification process, often leading to chemically stabilized peaty soils failing to achieve the desired engineering performance [7,8] The inhibitory effects of organic matter on soil stabilization arise from several mechanisms: i) Organic acids (e.g., humic acid and fulvic acid) contained in peaty soil lower the stabilized soil pore solution pH, thereby hindering the hydration reaction of cement [9]; ii) Humic acid readily reacts with Ca^{2+} to form calcium humate [10], while fulvic acid tends to reacts with Al^{3+}, potentially disrupting cement hydration products and decomposing calcium aluminate hydrate crystals [11]; iii) Humus adsorbs onto and encapsulates the surface of cement particles, thereby delaying hydration and pozzolanic reactions [12,13]; and iv) A high w_u reduces mineral soil particle proportions, weakening the soil skeleton and limiting pozzolanic reactions [14]. To enhance the applicability of chemical solidification methods for peaty soils, researchers and engineers have adopted several strategies: 1) Incorporation of specialized admixtures, such as chlorides, sulfates, and triethanolamine [15,16,17], which engage in ion exchange and complexation reactions with organic matter to reduce the negative impact of organic acids on cement solidification. For example, competing with organic acids for Ca^{2+} in the cementitious system or binding to active groups of humic/ fulvic acids, to reduce the negative impact of organic acids on cement hydration; 2) Utilization of cost-effective industrial by-products (e.g., silica fume [18], coffee husk ash and coconut fiber [19], slag and waste tire shreds [20]) to partially or entirely replace cement not only reduces overall solidification costs, but also lowers greenhouse gas emissions and enhances the reutilization of waste materials; 3) Blending peaty soil with non-organic soils (e.g., clay soil [8], manufactured sand [21]) to lower the absolute w_u and enhance the effectiveness of chemical reactions involved in solidification. These advancements have enabled chemically stabilized peaty soil to meet essential engineering requirements. Despite the challenges associated with high organic matter content, the chemical solidification method remains a preferred solution for the large-scale resource utilization of OM, owing to its technical maturity, construction convenience, and cost-effectiveness.

Phosphogypsum (PG) is the primary by-product of the wet-process production of phosphoric acid. Approximately 4.5–5.0 tons of PG are generated for every ton of phosphoric acid produced [22,23]. Global annual PG production is estimated to exceed 100 million tons and continues increasing at approximately 6 % per year. The cumulative worldwide stockpile has now surpassed 30 billion tons
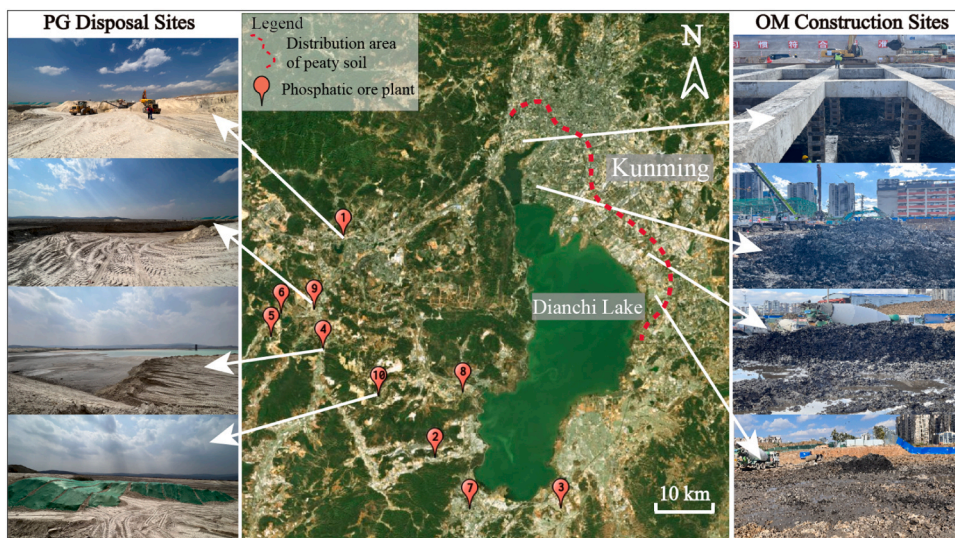

Fig. 1. Distribution of peaty soil strata and PG storage yards in Kunming City.

[24]. However, the vast majority of PG remains stockpiled in centralized locations, resulting in significant land resource occupation and posing potential environmental risks due to the presence of harmful constituents [25,26]. Solidifying and modifying PG for use as a geotechnical filler is considered an effective approach for promoting its large-scale utilization. As highlighted in a review [27], PG-based geotechnical fillers have been applied in various contexts, including highway embankment filling materials, mine pit backfill materials, and other engineering applications. In such applications, PG is typically blended with binding agents (e.g., cement, lime, fly ash), excavated muck, or other solid waste materials (e.g., red mud, slag) to achieve the objective of modifying and enhancing its engineering properties, and it is seldom used as the only stabilizing agent [28,29,30,31].

Kunming, the capital city of Yunnan Province, is located in southwestern China and is one of the few cities worldwide where deep layers of peaty soil exist beneath its urban area. According to a preliminary survey, well-developed layers of peat, peaty soil, and organic soil [32] have been identified in the shallow subsurface (0–30 m in depth) across more than one-third of the main urban area (approximately 300–520 km²), primarily located north of Dianchi Lake. As shown in Fig. 1, these areas are situated between the red dotted line and Dianchi Lake. Over the past two decades, rapid urban development has significantly intensified the utilization of underground space. As a result, a substantial amount of organic-rich muck has been generated from various excavation activities, including deep foundations, deep foundation pits, utility tunnels, shield tunnels, and other infrastructure projects. While a limited amount of relatively pure OM has been repurposed as soil for municipal landscaping or agricultural substrate, a substantial portion remains stockpiled in disposal sites. Currently, the annual production of engineering muck in Kunming City exceeds several million tons, with 51 muck disposal sites either decommissioned or currently in operation. Additionally, Kunming possesses abundant phosphate rock resources, with proven reserves of approximately 1.02 billion tons, accounting for over 14 % of China's total. According to statistics from the Kunming Municipal Government, the city hosts more than a dozen wet-process phosphoric acid production enterprises. As shown in Fig. 1, the red indicators mark at least ten phosphate ore plants located west of Dianchi Lake. Collectively, these facilities generated approximately 19.03 million tons of PG in 2023. Although the comprehensive utilization rate of PG has reached 70.62 %, primarily through applications such as gypsum boards manufacturing and its use as backfill material for underground goafs [33] and subgrade fill materials [34], a substantial volume of PG remains to be stockpiled in tailing ponds [35]. Both muck yards and tailing ponds occupy significant land areas and pose potential environmental pollution risks. As a result, OM and PG have become two major categories of solid waste constraining urban development in Kunming, highlighting the urgent need for effective strategies to promote their large-scale resource utilization.

Controlled Low-Strength Material (CLSM) is a highly flowable backfill material capable of self-compaction under conditions of little or no vibration [36]. It is particularly well-suited for backfilling applications in confined or difficult-to-access spaces, such as foundation pits, wide trenches, and municipal pipeline excavations [37,38,39,40]. CLSM is typically prepared using binders, fine aggregates, and water. Common binding materials include Ordinary Portland cement (OPC) and fly ash (FA). In addition to conventional sand, various solid waste materials can be partially or fully used as substitutes for fine aggregates [41,42]. These alternatives include industrial by-products (e.g., cement kiln dust [43,44], slag [45,46,47,48], quarry stone powder [49]), different types of engineering mucks (e.g., dredged mud [50,51], expansive soil [52], collapsible loess [53], shield muck [54,55]), construction demolition waste [56], mining waste [57,58]. and agricultural residues [59]). Since its inception, CLSM has evolved from the use of single-type fine aggregates to the incorporation of composite fine aggregates. The utilization of composite fine aggregates comprising engineering mucks and industrial by-products has been extensively studied and has demonstrated satisfactory engineering performance. Representative examples include silt-tire crumb mixtures [60], kaolin-bottom ash mixtures [61], construction muck-fly ash mixtures [62], silt-red mud mixtures [63], dredged soil-slag mixtures [64], collapsible loess-crushed stone soil mixtures [53], and Titanium gypsum-construction waste composite fine aggregate [65,66]. Due to the ability of chemical reaction products formed between the binding materials and the matrix to effectively reduce the leaching of harmful substances, even materials containing hazardous components have been investigated as potential fine aggregates. For instance, Kim et al. [62] examined the reuse of arsenic-rich tailings in CLSM formulations. Wang et al. [67] assessed the feasibility of utilizing contaminated sediments for CLSM production. Razak et al. [68] demonstrated that incineration bottom ash, when incorporated into CLSM, can significantly reduce the leaching of harmful substances. Overall, there are no stringent specifications for fine aggregates, provided that the resulting CLSM satisfies relevant performance criteria through standardized testing [55,69]. Given that fine aggregates typically comprise over 80 % of the dry materials in CLSM, their production offers a promising pathway for the large-scale resource utilization of solid waste materials.

Although the ACI 229R–13 [36] suggests caution when using clayey and organic soils as fine aggregates, due to potential challenges such as poor mix uniformity and curing difficulties, recent studies have indicated that, through the incorporation of admixtures and appropriate mix design, even high-plasticity clay [70] and organic soils [64,71] can be effectively utilized to produce CLSM with desirable properties. Based on the concept of "treating waste with waste" [72,73], this study proposes the utilization of waste organic muck (OM) and phosphogypsum (PG) to develop composite fine aggregates for the production of Controlled Low Strength Material (OP-CLSM). The feasibility of this method is supported by the following considerations: 1) As a low-grade backfill material, CLSM imposes relatively lenient restrictions on the organic matter content (w_u) of the matrix; 2) Although high w_u is a critical factor contributing to inadequate solidification, the incorporation of PG effectively lower the absolute w_u of the composite fine aggregate; 3) Numerous researches have shown that PG, widely used as a cement admixture, can mitigate the adverse effects of organic matter and enhance the solidification performance [74,75]; 4) Given its fine-grained soil characteristics, OM can address issues such as high bleeding rates when PG is used as the only fine aggregate in CLSM. Based on these deliberations, the development of OP-CLSM using OM and PG offers a promising strategy that can substantially contribute to sustainable local economic development.

However, based on a comprehensive literature review, most muck employed as fine aggregates for CLSM preparation consists of non-organic soils, with no documented instance of directly using organic muck (OM). To provide a scientific foundation for the development of OP-CLSM, this study aims to achieve the following specific research objectives: 1) Systematically evaluate the

engineering properties and environmental safety of OP-CLSM, thereby establishing the feasibility of utilizing OM and PG as composite fine aggregates for CLSM; 2) Investigate the effects of the OM-to-PG mass mixing ratio (M_{OM}: M_{PG}), the w_u of OM, the cement-to-fly ash mixing ratio (a_{OPC}: a_{FA}), and the types of admixtures (PCE, CaCl$_2$, and TEA) on the performance of OP-CLSM. This investigation will facilitate the determination of suitable compositions of fine aggregate and binders, as well as the selection of appropriate admixtures for OP-CLSM; 3) Analyze the mineral composition and microstructure of OP-CLSM through X-ray diffraction (XRD) and scanning electron microscopy (SEM), thereby elucidating its binding mechanism.

2. Materials

2.1. Fine aggregates

2.1.1. Organic Muck (OM)

Four types of OM samples with varying organic matter contents (w_u) are collected from four excavation projects within the urban area of Kunming. These sites included deep building foundation pits, subway station foundation pits, municipal utility tunnels, and river channel widening projects. The basic physical properties of the collected samples are summarized in Table 1. Specifically, water content is determined using the oven-drying method at a drying temperature of 55 °C [76,77]. The liquid limit and plastic limit are measured following the combined determination method specified in GB/T 50123–19 [78]. Additionally, the w_u is assessed using the ignition method [79], while the residual fiber content is determined using the wet sieving method [80]. As shown in Table 1, these soil samples exhibit high initial water content ($w_0 = 166.1 – 211.7$ %), high organic matter content ($w_u = 14.41 – 53.3$ %), and weak acidity (pH $= 4.9 – 5.7$). In contrast, residual fiber content is relatively low across all samples, indicating that they belong to amorphous peaty soils [81].

Generally, fine-grained soils are not recommended as fine aggregate for CLSM preparation due to their tendency to resist dispersion in water and their difficulty in forming a uniformly mixed slurry. Therefore, a self-developed preliminary dispersibility test is conducted to evaluate the behavior of OM when immersed in water. As shown in Fig. 2, after the natural soil mass is left to stand in water for approximately two minutes, partial disintegration is observed. Subsequent stirring with a glass rod for about two minutes results in the formation of a uniform slurry. This behavior can be attributed to the porous and loose structure of organic matter [3,14], which exhibits strong water adsorption capability, thereby promoting rapid dispersion upon immersion. As a result, OM can be directly mixed with water and dispersed into a slurry state without the need for pre-treatment processes such as air drying, crushing, or screening. This advantageous characteristic supports OM viability as a fine aggregate for CLSM.

2.1.2. Phosphogypsum (PG)

In this study, PG is used as a composite fine aggregate in the preparation of CLSM. The PG used in this study is sourced from the storage yard of Yunnan Yuntianhua Co., Ltd., where it had been stockpiled for over two years. According to the particle size distribution test results obtained by a laser particle size analyzer, PG primarily consists of silt particles. Details regarding its material composition, including chemical composition and physical properties, are provided in Tables 2 and 3.

2.2. Binders and admixtures

Ordinary Portland cement (OPC) Grade 42.5 (Specific gravity: 3.12, Specific area: 350 m²/kg, 45 μm sieve residue: 5.0 %) and Fly Ash (FA) (Specific gravity: 2.40, Specific area: 380 m²/kg, 45 μm sieve residue: 17.5 %) are selected as the binders. The OPC used is manufactured and supplied by Kunming Dongji Cement Co., Ltd., while the FA is Class II power plant fly ash produced by Gongyi Lanke Environmental Protection Water Purification Material Co., Ltd. The primary chemical compositions of PG, OPC, and FA are summarized in Table 3. As shown in Table 3, OPC is dominated by CaO, while FA is rich in SiO$_2$ and Al$_2$O$_3$, as a typical pozzolanic material, and both play important roles in the cementitious mixture.

To further enhance the engineering performance of the OP-CLSM material, three chemical admixtures are incorporated: Polycarboxylate superplasticizer (PCE), a high-efficiency water-reducing agent; Calcium chloride anhydrous (CaCl$_2$), an early-strength agent; and Triethanolamine (TEA, C$_6$H$_{15}$NO$_3$, Purity≥99.5 %, relative density ρ_{20}=1.120–1.130), both a retarder and later strength enhancer in concrete. All admixtures are supplied by Sinopharm Chemical Reagent Co., Ltd., Shanghai.

Table 1

Basic physical properties of OM samples.

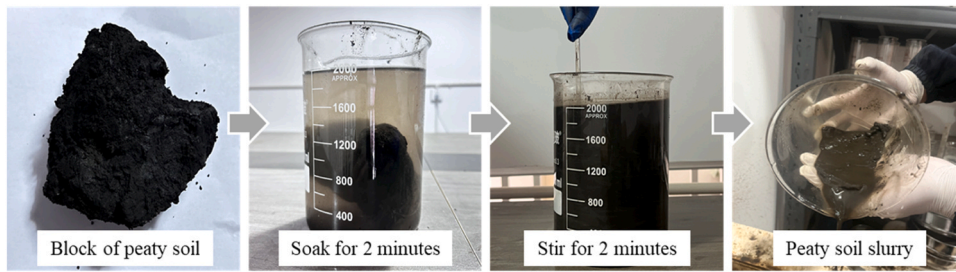| No. of Sampling site	Initial water content/%	Liquid limit/%	Plasticity limit	Organic matter content/%	Fiber content/%	pH
1	166.1	175.5	90.2	14.41	0.0	5.7
2	194.4	234.6	98.1	20.65	0.1	5.6
3	188.8	316.9	133.4	37.91	0.3	5.2
4	211.7	412.5	165.6	53.30	1.2	4.9

Fig. 2. Dispersibility test of peaty soil immersed in water.

Table 2
Basic physical properties of PG.

Specific gravity	Initial water content/%	Particles < 75 μm (%)	Particles < 5 μm (%)	pH	Color
2.35	3.3	83.0	12.3	5.2	gray

Table 3
Main chemical compositions of materials.

Oxide content	Phosphogypsum (PG)	Cement (OPC)	Fly ash (FA)
SiO_2	11.19	19.99	45.99
CaO	38.66	59.35	5.38
Al_2O_3	0.56	5.85	39.30
Fe_2O_3	0.25	4.65	4.78
MgO	1.22	3.07	0.39
SO_3	45.70	3.18	0.64
TiO_2	0.09	1.49	1.76
F	0.75	-	-
P_2O_5	1.21	-	-
others	0.37	2.42	1.49

Table 4
Mix design schemes and IDs for all OP-CLSM specimens.

Mix ID	Binder	Fine aggregate	Density(kg/m^3)
(a) Analyze the influence of M_{OM}: M_{PG}			
OM0PG80	12 %OPC+ 8 %FA	80 %PG	1708
OM20PG60 (w_u=53.30 %)		60 %PG+ 20 %OM (w_u=53.30 %)	1571
OM40PG40 (w_u=53.30 %)		40 %PG+ 40 %OM (w_u=53.30 %)	1523
OM60PG20 (w_u=53.30 %)		20 %PG+ 60 %OM (w_u=53.30 %)	1501
OM80PG0 (w_u=53.30 %)		80 % OM (w_u=53.30 %)	1471
OM20PG60 (w_u=20.65 %)		60 %PG+ 20 %OM (w_u=20.65 %)	1645
OM40PG40 (w_u=20.65 %)		40 %PG+ 40 %OM (w_u=20.65 %)	1562
OM60PG20 (w_u=20.65 %)		20 %PG+ 60 %OM (w_u=20.65 %)	1531
OM80PG0 (w_u=20.65 %)		80 % OM (w_u=20.65 %)	1436
(b) Analyze the influence of w_u			
OM40PG40 (w_u=14.41 %)	12 %OPC+ 8 %FA	40 %PG+ 40 %OM (w_u=14.41 %)	1568
OM40PG40 (w_u=20.65 %)		40 %PG+ 40 %OM (w_u=20.65 %)	1562
OM40PG40 (w_u=37.91 %)		40 %PG+ 40 %OM (w_u=37.91 %)	1554
OM40PG40 (w_u=53.30 %)		40 %PG+ 40 %OM (w_u=53.30 %)	1523
(c) Analyze the influence of a_{OPC}: a_{FA}			
C8FA12	8 %OPC+ 12 %FA	40 %PG+ 40 %OM (w_u=53.30 %)	1523
C10FA10	10 %OPC+ 10 %FA		1527
C12FA8	12 %OPC+ 8 %FA		1523
C14FA6	14 %OPC+ 6 %FA		1557
C16FA4	16 %OPC+ 4 %FA		1574
(d) Analyze the influence of admixture types			
PCE	12 %OPC+ 8 %FA+ 0.4 %PCE	40 %PG+ 40 %OM (w_u=53.30 %)	1479
$CaCl_2$	12 %OPC+ 8 %FA+ 0.4 %$CaCl_2$		1495
TEA	12 %OPC+ 8 %FA+ 0.4 %TEA		1522

Note: w_u: organic matter content; OPC: ordinary Portland cement; FA: pulverized fly ash; PG: phosphogypsum; OM: organic muck; PCE: poly-carboxylate superplasticizer; $CaCl_2$: calcium chloride; TEA: triethanolamine.

3. Methodology

3.1. Mix design

To investigate the effects of key factors on properties of OP-CLSM, including the mass mixing ratio of OM to PG (M_{OM}: M_{PG}), the w_u of OM, the mixing ratio of OPC to FA (a_{OPC}: a_{FA}), and the types of admixtures (PCE, $CaCl_2$, and TEA), four groups of comparative mix designs are formulated. All mix designs maintained a constant mass ratio of stabilizers to dry mixed fine aggregates at 1:4 (i.e., 20 % stabilizers + 80 % fine aggregates). Table 4 presents the complete mix design schemes and IDs for all OP-CLSM specimens. The detailed mix design configurations are outlined as follows:

- Group (a): To analyze the influence of M_{OM}: M_{PG} on the properties of OP-CLSM, five different fine aggregate mixing ratios are established: M_{OM}: M_{PG} = 0:80, 20:60, 40:40, 60:20, and 80:0. Two types of OM with high and low organic matter content (w_u=53.30 % and 20.65 %, respectively) are used. The dosage of the binders is fixed at 12 % OPC and 8 % FA. This group includes a total of nine specimen types.
- Group (b): To evaluate the effect of w_u of OM, four types of OM with varying w_u (14.41 %, 20.65 %, 37.91 %, and 53.30 %) are utilized to prepare the fine aggregate. The fine aggregate proportion is fixed at 40 % OM and 40 % PG, and the binder dosage is maintained at 12 % OPC and 8 % FA. This group comprises four specimen types.
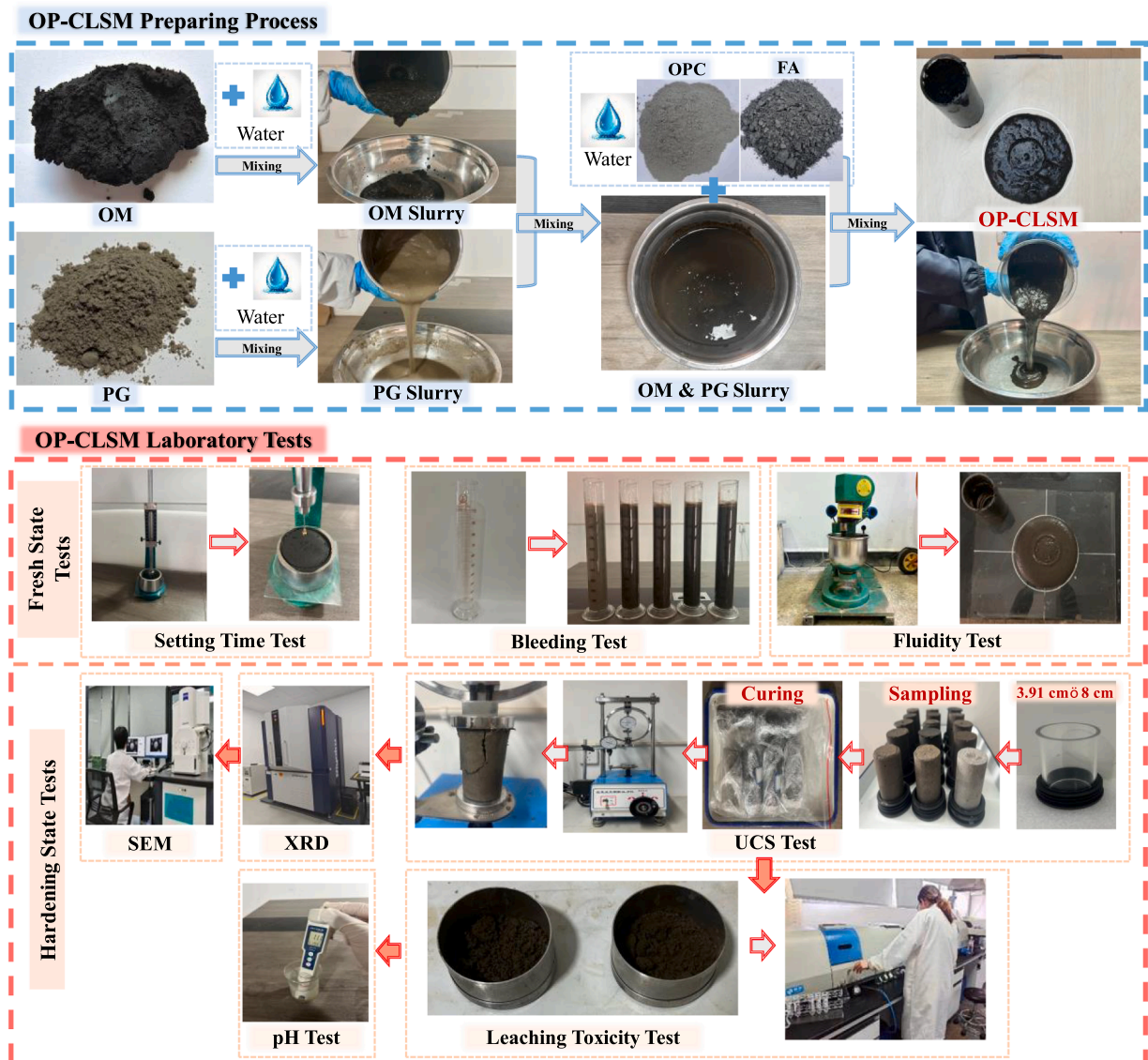

Fig. 3. Preparation and experimental procedures of OP-CLSM.

- Group (c): To assess the impact of the binder dosage and composition, five different binder mixing ratios are set: a_{OPC}: a_{FA} = 8:12, 10:10, 12:8, 14:6, and 16:4. The fine aggregate proportion is fixed at 40 % OM and 40 % PG (with w_u=53.30 %). This group includes five specimen types.
- Group (d): To examine the influence of admixture type on OP-CLSM properties, three types of admixtures are respectively added to separate mixes: they are polycarboxylate superplasticizer (PCE), calcium chloride (CaCl₂), and triethanolamine (TEA). The admixture dosage is 0.4 % of the cement mass. The fine aggregate proportion is fixed at 40 % OM and 40 % PG (with w_u=53.30 %), and the binder dosage remained at 12 % OPC and 8 % FA. This group includes three specimen types.

3.2. OP-CLSM preparation

The laboratory preparation process of OP-CLSM involves mixing, molding, and curing. Initially, OM is placed into a planetary mixer along with a pre-determined amount of water and stirred for two minutes. The water content is adjusted to 1.2 times the liquid limit (w_L) of OM to form a slurry. Next, PG is added along with additional water (equal to 50 % of the PG mass) and stirred for an additional two minutes to obtain a uniform fine aggregate slurry. Subsequently, the binder slurry (including admixtures) is added in one batch, with the water-to-solid ratio controlled at 0.35, and the entire mixture is stirred for a further two minutes to ensure uniformity. The resulting mixed slurry is poured into molds and allowed to set for 48 h prior to demolding. Finally, the specimens are wrapped airtight with plastic film and cured in a curing chamber maintained at a temperature of 20 ± 2°C and a humidity of 90 %. The preparation and testing procedures for OP-CLSM are illustrated in Fig. 3.

3.3. Test Methods

A series of laboratory tests were conducted to evaluate the engineering properties and environmental safety of OP-CLSM in both its fresh and hardened states comprehensively (Table 5). The performance of the fresh-state slurry is assessed through flow testing, bleeding rate measurement, and setting time determination. For the hardened OP-CLSM, unconfined compressive strength (UCS) tests are conducted to evaluate mechanical performance. The mineralogical characteristics and microstructure features are investigated using X-ray diffraction (XRD) and scanning electron microscopy (SEM), respectively. Environmental safety assessments involve pH testing and acetic acid leaching tests to determine the potential harmful substance release.

3.3.1. Fresh-state OP-CLSM properties tests

Flow Tests: The flowability of OP-CLSM is evaluated in accordance with ASTM D6103M−17 [82] using an open-ended acrylic cylinder with a diameter of 7.5 cm and a height of 15 cm. The procedure is as follows: The mold is placed on a flat glass plate, and freshly mixed OP-CLSM is poured into the mold. The outer wall of the mold is gently tapped to eliminate air pockets, and the surface is leveled with a spatula. After standing for 5 s, the mold is lifted vertically, allowing the material to spread freely. The maximum and minimum diameters of the spread material are measured, and their average is recorded as the flowability index.

Bleeding Tests: The bleeding behavior of OP-CLSM is evaluated in accordance with ASTM C940−22 [83]. The freshly prepared mixture is poured into a 1000 mL graduated cylinder, with the volume controlled at 800 mL. The cylinder is completely wrapped with plastic film to prevent moisture loss. During the test, the accumulation of bleed water on the surface is continuously monitored and recorded until no further bleeding is observed. The final bleeding rate is determined based on the total volume of bleed water collected.

Setting Time Tests: The setting time of OP-CLSM is determined in accordance with Chinese Standard GB/T 1346−11 [84], and the American Standard ASTM C191−21 [85]. The freshly mixed OP-CLSM is poured into a metal container and subsequently placed in a constant temperature and humidity chamber maintained at 20°C and 50 % relative humidity. Prior to each measurement, the sample is removed from the chamber, and the setting time is assessed following the standard procedure. The elapsed time from the start of mixing to the point at which the sample met the defined setting criteria is recorded as the setting time.

3.3.2. Hardened OP-CLSM properties tests

Unconfined Compressive Strength (UCS) Tests: For the UCS test, cylindrical specimens are prepared by pouring freshly mixed OP-

Table 5
Summary of the OP-CLSM comprehensive test program.

Stages	Test items	Curing time	Referred test standards
OP-CLSM preparation	Material Preparation and Mixing	-	-
	Molding and Demolding	48 h	-
	Curing	7 d、28 d	-
Fresh-state OP-CLSM properties tests	Flow Tests	-	ASTM D6103M−17
	Bleeding Tests	-	ASTM C940−22
	Setting Time Tests	-	GB/T 1346−11 (2011)；ASTM C191−21 (2021)
Hardened OP-CLSM properties tests	UCS Tests	7 d、28 d	ASTM D2166/D2166M−24
	XRD Tests	28d	-
	SEM Tests		
Environmental safety assessment tests	pH Tests	0d、7d、28 d	ASTM D4972−19
	Acetic Acid Leaching Tests	28 d	EPA Method 1311

CLSM into molds with dimensions of 3.91 cm in diameter and 8 cm in height. After 48 h of setting, the specimens are demolded and wrapped with plastic film. Subsequently, the sealed specimens are cured in an environment-controlled chamber at a temperature of 20 $\pm$ 2°C and a relative humidity of 95 %. UCS tests are conducted at specified curing ages of 7 and 28 days in accordance with ASTM D2166/D2166 M–24 [86], using an unconfined compression testing machine with a constant loading rate of 2 mm/min. Each group of samples includes three parallel samples.

X-ray Diffraction (XRD) and Scanning Electron Microscopy (SEM) Analysis: After the UCS test, powder samples and square samples (1 cm × 1 cm × 1 cm) are collected from the failure surfaces of the OP-CLSM specimens, respectively. Prior to XRD testing, the samples are first ground into powder, dried in an oven at 105°C, and then sieved through a 200-mesh sieve ($\approx$75 µm aperture) to obtain samples with uniform fineness. The XRD tests are conducted using a Rigaku SmartLab SE X-ray diffractometer. The XRD test is performed within a 2θ range of 5° to 90°, and the obtained diffraction patterns are subjected to phase analysis and identification using JADE 6.0 software. Before SEM analyses, the broken specimens are trimmed into square flakes with side lengths less than 10 mm and dried in an oven at 105°C. Subsequently, the surface of the samples is sputter-coated with a gold layer (approximately 20–30 nm thick) to enhance their electrical conductivity. The microstructure observation is carried out using a VEGA-3SBH scanning electron microscope.

3.3.3. Environmental safety assessment tests

pH Tests: The pH value of OP-CLSM is determined in accordance with ASTM D4972–19 [87] using a calibrated pH meter provided by Lichen Technology Co., Ltd. The procedure involves air-drying the hardened OP-CLSM samples, followed by crushing and sieving through a 2 mm sieve. Subsequently, 10 g of the sieved OP-CLSM is then mixed with 50 mL of distilled water in a glass container. The mixture is vibrated and stirred for three minutes, then left to stand for 1 h before measuring the pH value. The temperature of the solution, ranging from 19.6 to 23.8°C, is monitored during the measurement.

Acetic Acid Leaching Tests: To evaluate the leaching behavior of harmful substances in OP-CLSM and assess potential environmental risks during service life, an acetic acid buffer solution extraction test is conducted in accordance with the EPA Method 1311 [88], which recommends the horizontal oscillation method for solid waste leaching. The procedure is as follows: Following the 28-day UCS test, the cured OP-CLSM specimens are oven-dried at 45°C, further crushed, and sieved through a 3 mm sieve. 2 g of the sieved OP-CLSM sample are mixed and soaked in a polyethylene leaching test tube containing 40 mL of acetic acid buffer solution. The mixture is shaken horizontally at a speed of 110 cycles per minute for 8 h at room temperature using a reciprocating shaker, and is subsequently allowed to stand undisturbed for 16 h. The supernatant is filtered through a 0.45 µm membrane filter to obtain the leachate. For comparative purposes, an identical acetic acid leaching procedure is performed on untreated PG. The concentrations of heavy metals and non-metallic pollutants in the leachate are analyzed using an Inductively Coupled Plasma Optical Emission Spectrometer (ICP-OES, PerkinElmer Optima 8000).
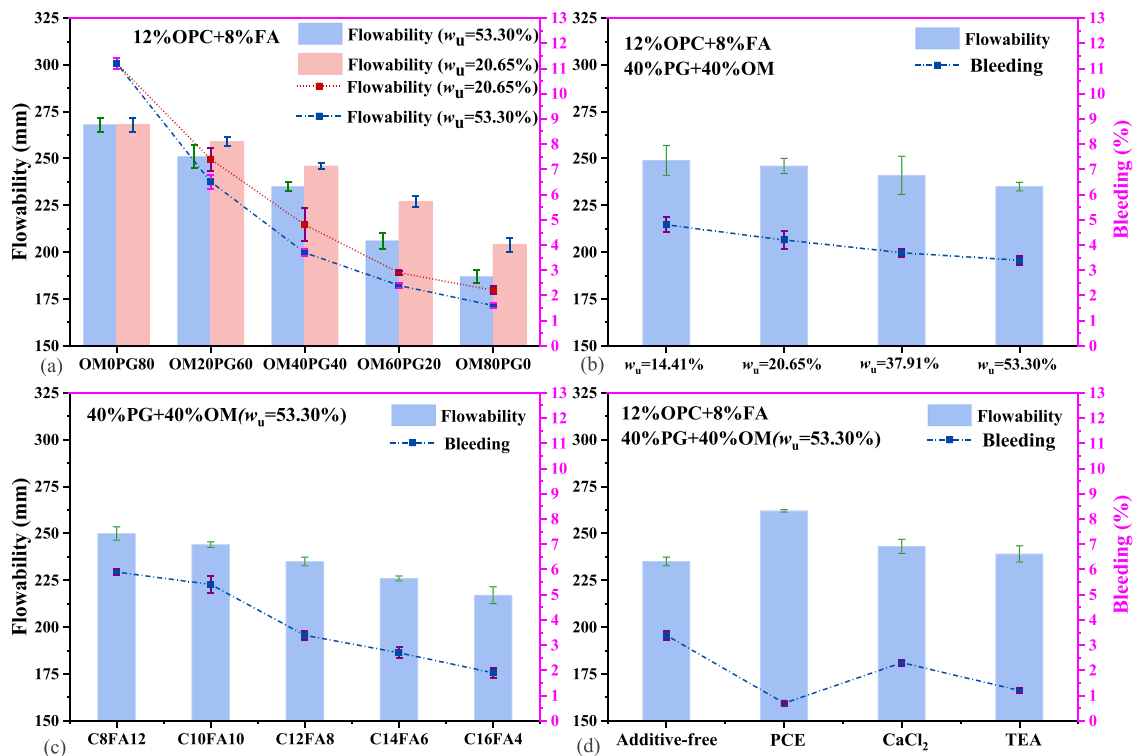

Fig. 4. Flowability and bleeding rate of OP-CLSM under different effect indexes. M_{OM}: M_{PG}; (b) w_u; (c) a_{OPC}: a_{FA}; (d) Types of admixtures.

4. Results and discussion

4.1. Fresh-state OP-CLSM properties

4.1.1. Flowability and bleeding

The ability to achieve self-leveling and self-compacting behavior is a defining characteristic that sets CLSM apart from conventional backfill materials, which require adequate flowability. Generally, the reasonable flowability range for CLSM is between 150 and 300 mm [36,89]. The bleeding rate is another critical indicator for evaluating the workability of CLSM, which reflects the extent of water separation from the mixture after placement. Controlling the bleeding rate is crucial to minimizing post-construction settlement and deformation. According to existing specifications, the bleeding rate of CLSM within 120 min should remain below 5 % [62,90]. Some researchers propose a broader acceptable range, typically between 0.4 % and 7.2 % [52,68,91]. In general, as CLSM flowability increases, so does the bleeding rate, underscoring the importance of identifying a suitable balance to meet performance requirements.

Fig. 4(a) illustrates the influence of M_{OM}: M_{PG} on the flowability and bleeding rate of OP-CLSM under a fixed stabilizer dosage (12 % OPC + 8 % FA). As shown, increasing the proportion of OM, while correspondingly decreasing PG, results in a significant reduction in both flowability and bleeding rate of OP-CLSM. Additionally, a higher proportion of OM with a higher w_u leads to a reduction in both flowability and bleeding rate. For instance, the flowability of OP-CLSM with OM0PG80 is 268 mm, with a bleeding rate of 11.2 %. In contrast, when OM is increased to 80 % with w_u= 20.70 % (OM80PG0), flowability drops to 204 mm and the bleeding rate to approximately 2.2 %. For the same OM proportion but with w_u= 53.30 % (OM80PG0), flowability further decreases to 187 mm, with the bleeding rate reduced to around 1.6 %.

Fig. 4(b) depicts the effect of OM with different w_u on the flowability and bleeding rate of OP-CLSM, under fixed conditions of fine aggregate composition (40 % OM + 40 % PG) and binder dosage (12 % OPC + 8 % FA). The results indicate that as the w_u of OM increases, both flowability and bleeding rate exhibit a slight decline. Specifically, when w_u increases from 14.41 % to 53.30 %, the flowability decreases from 249 mm to 235 mm, while the bleeding rate declines from 4.8 % to 3.4 %, confirming the strong water-retention effect of high-organic matter content OM on the workability of OP-CLSM. These test trends align with those observed in CLSM, which incorporates non-organic muck as a fine aggregate. For instance, Zhu et al. [53] reported that increasing the proportion of waste expansive soil in the fine aggregate leads to a reduction in CLSM flowability. Similarly, Do et al. [91] found that a higher proportion of dredged sediment results in a gradual decrease in bleeding rate. Zhao et al. [55] demonstrated that the incorporation of shield tunneling muck significantly diminishes CLSM flowability. These findings support the conclusion that mineral clay particles and organic matter in OM possess substantially greater water adsorption capabilities than PG, whose particle size distribution is closer to
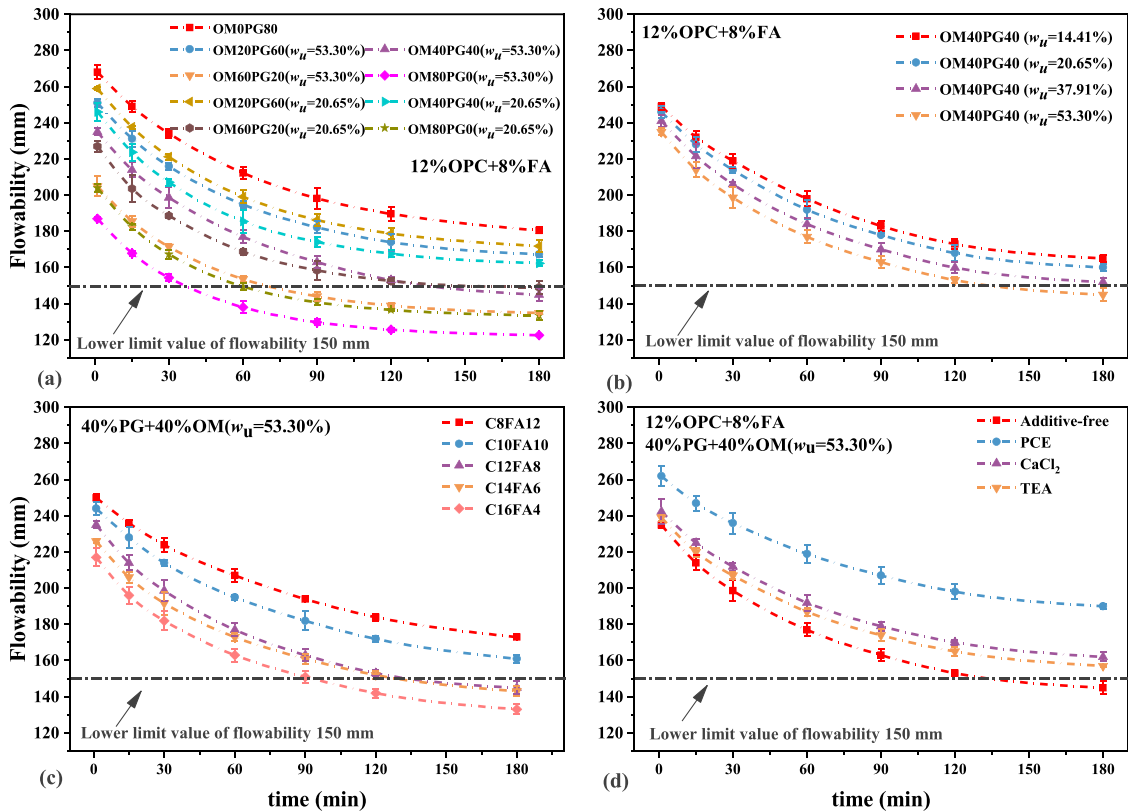

Fig. 5. Time-dependent changes in OP-CLSM flowability. M_{OM}: M_{PG}; (b) w_u; (c) a_{OPC}: a_{FA}; (d) Types of admixtures.

that of silt. In particular, the organic fraction of OM exhibits a superior water adsorption capacity compared to common clay minerals (especially montmorillonite), which adsorbs several times its own weight in water. This marked difference in water retention between OM and PG underlies the observed variations in flowability and bleeding behavior of OP-CLSM.

Fig. 4(c) illustrates the effect of varying the a_{OPC}: a_{FA} on the flowability and bleeding rate of OP-CLSM. As the a_{OPC}: a_{FA} increases, both flowability and bleeding rate decrease, a trend consistent with the findings reported by Salini et al. [92]. This mechanism stems from the combined effects of more cement hydration products and the ball-bearing effect of fly ash: a higher OPC proportion increases early-stage hydration products (e.g., C-S-H gel), raising the internal friction of the CLSM system and reducing its flowability; simultaneously, the spherical morphology of fly ash enables its ball-bearing effect [93] to lower inter-particle friction in the CLSM matrix, and less FA weakens this lubrication, further worsening the decline in flowability.

Fig. 4(d) depicts the influence of different admixtures (PCE, CaCl₂, and TEA) on the fresh-state properties of OP-CLSM. Among them, PCE shows the most significant enhancement in flowability and bleeding rate. PCE, acting as a high-efficiency water-reducing agent, generates strong electrostatic repulsion and steric hindrance effects on the surface of cement particles, thereby reducing particle aggregation and promoting dispersibility [64]. CaCl₂, functioning as an early strength agent, also improves flowability and bleeding performance of OP-CLSM. This is primarily due to its electrolyte properties, which partially mitigate particle adsorption. TEA, commonly used as a retarder and later strength enhancer in concrete, has a negligible effect on the flowability of OP-CLSM but effectively improves bleeding performance.

In summary, the flowability of all OP-CLSM prepared in this study meets the relevant standards (150–300 mm) [36]. When the proportion of OM in the fine aggregate exceeds 20 % (12 % OPC + 8 % FA), the bleeding rate of OP-CLSM all complies with the relevant standards (0.4–7.2 %) [52,68,91].

Fig. 5 illustrates the time-dependent changes in OP-CLSM flowability. It is evident from the figure that, similar to other CLSM types [52,94], OP-CLSM also displays a trend of decreasing flowability with prolonged time, which is attributed to the gradual hardening of the mixed slurry driven by cement hydration. A comprehensive analysis of Fig. 5(a-d) reveals that the M_{OM}: M_{PG} ratio, w_u, a_{OPC}: a_{FA} ratio, and admixture types have no significant impact on the pattern of OP-CLSM flowability decreasing over time; within the time range of 1–180 min, the differences in the degree of flowability decline among OP-CLSM with different mix proportions are relatively small. However, significant differences in initial flowability lead to substantial variations in the engineering adaptability of OP-CLSM with different mix proportions. For example, with fixed binders (12 % OPC + 8 % FA), OP-CLSM with OM80PG0 ($w_u = 53.30$ %) has an initial flowability of 187 mm, dropping below the lower limit value of flowability (150 mm) at approximately 30 min; in contrast, OM40PG40 ($w_u = 53.30$ %) with an initial flowability of 270 mm takes 120 min to reach this standard limit.
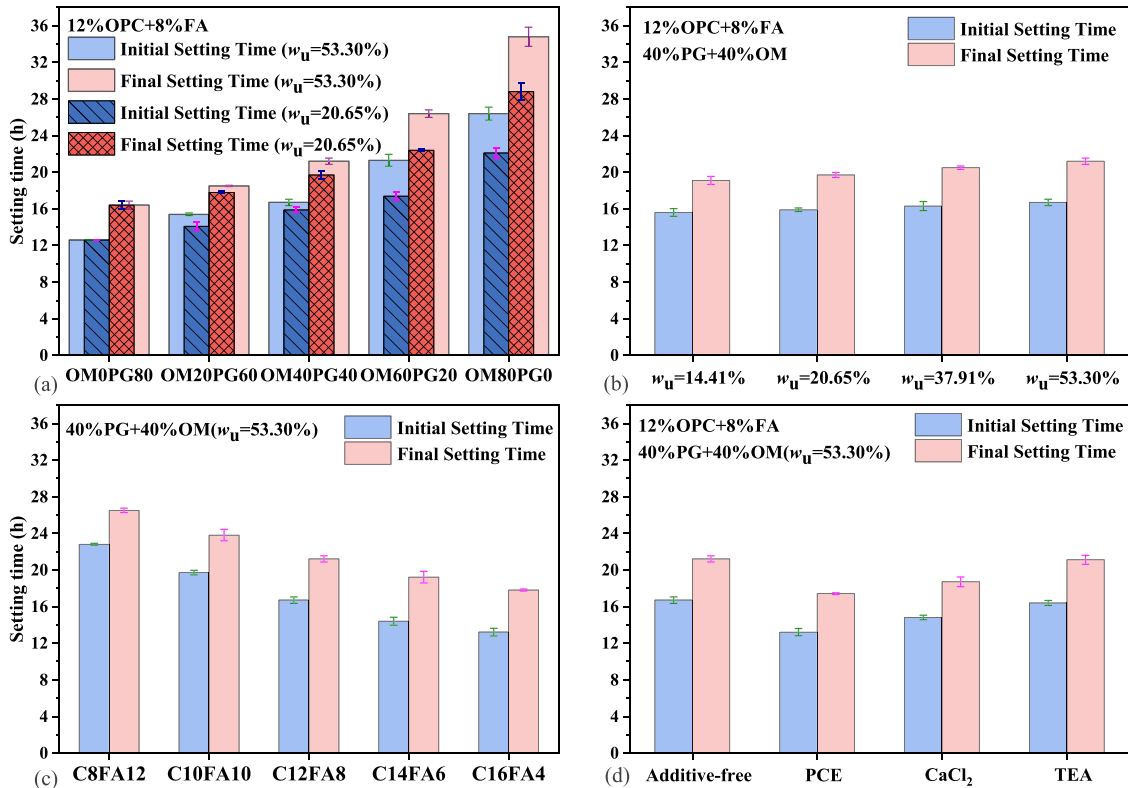

Fig. 6. Initial and final setting time of OP-CLSM under different effect indexes. (a) M_{OM}: M_{PG}; (b) w_u; (c) a_{OPC}: a_{FA}; (d) Types of admixtures.

4.1.2. Setting time

Setting time is a critical parameter in CLSM applications, particularly for projects requiring rapid traffic restoration or timely follow-up construction. Generally, the final setting time of CLSM is expected to be within 24 h to meet construction schedule demands [44,95].

Fig. 6(a) illustrates the relationship between the M_{OM}: M_{PG} and the initial and final setting times of OP-CLSM. A clear upward trend is observed with increasing OM content. Specifically, for OM0PG80, the initial setting time is 12.6 h, and the final setting time is 16.4 h; whereas for OM80PG0, the initial and final setting times increase to 26.4 h and 34.8 h, respectively. Notably, when the OM proportion exceeds 60 %, the final setting time surpasses the acceptable 24-hour threshold. Its mechanism is the same as the one mentioned earlier, where the increase in OM content leads to a decrease in the flowability and bleeding rate of OP-CLSM. The water adsorption capacity of OM is significantly higher than that of PG, resulting in hydration delay and a prolonged setting time. This is also similar to the mechanism observed by Zhao et al. [55], where partial replacement of conventional sand with high fine-grained shield tunnel spoil increases the proportion of fine aggregate, leading to a prolongation of the setting time of CLSM.

Fig. 6(b) shows the effect of OM organic matter content (w_u) on setting time under fixed fine aggregate proportion conditions (40 % OM + 40 % PG) and a consistent binder dosage (12 % OPC + 8 % FA). The results indicate that as w_u increases, both the initial and final setting times are prolonged, further highlighting OM's retardation effect due to its water retention and organic constituents.

Fig. 6(c) presents the influence of the binders composition (a_{OPC}: a_{FA}) on setting behavior. Increasing the OPC content (while reducing FA) significantly shortens both setting times. As the OPC content increases from 8 % to 16 %, the initial setting time drops from 22.8 h to 13.2 h (a 42.1 % reduction), and the final setting time decreases from 26.5 h to 17.8 h (a 32.8 % reduction). These results align with the findings of Khadka et al. [96] and Wang et al. [21], who attribute this behavior to the increased formation of hydration products such as calcium silicate hydrate (C-S-H). As the OPC content increases, the generation of these products reduces the flowability of OP-CLSM and accelerates its transition into the setting state. This observation supports the previously discussed mechanism whereby higher OPC contents lead to lower flowability and bleeding rate in OP-CLSM.

Fig. 6(d) shows the effect of different admixtures (PCE, $CaCl_2$, and TEA) on the setting time of OP-CLSM. Among them, PCE exhibits the most significant reduction in both initial and final setting times, followed by $CaCl_2$ and then TEA. This trend is consistent with the findings reported by Wang et al. [71]. PCE enhances particle dispersion, $CaCl_2$ improves both flowability and bleeding rate, while TEA, commonly used as a set retarder, has the least influence on reducing setting time. The mechanism of triethanolamine (TEA), particularly its role as a retarding agent with minimal impact on setting time, will be the subject of further investigation in subsequent studies, with detailed results to be reported in future publications.
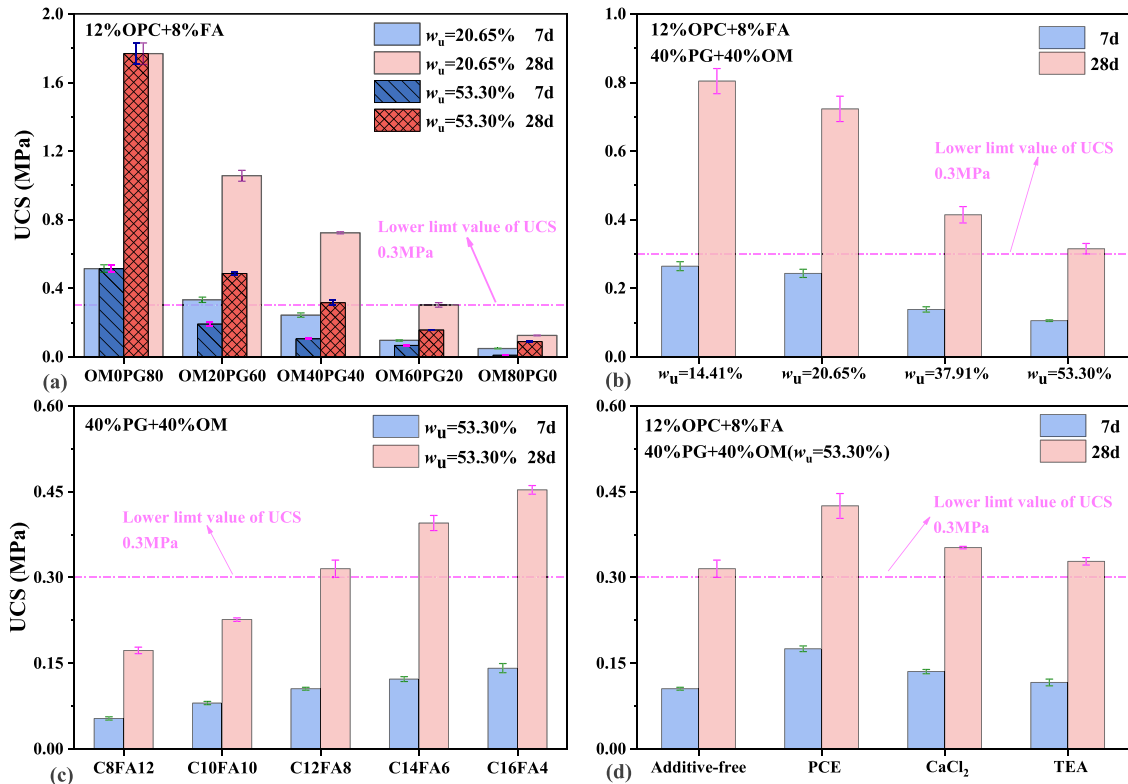

Fig. 7. UCS of OP-CLSM under different effect indexes. M_{OM}: M_{PG}; (b) w_u; (c) a_{OPC}: a_{FA}; (d) Types of admixtures.

4.2. Hardened OP-CLSM properties

4.2.1. Unconfined compression strength (UCS)

The strength of CLSM is a fundamental performance metric, particularly its unconfined compression strength (UCS) at 28 days. According to standard guidelines, the 28-day UCS should not be less than 0.3 MPa to ensure structural integrity, but also not exceed 8.3 MPa to retain excavability [36]. If manual excavation is required, the UCS should ideally remain below 0.7 MPa.

Fig. 7(a) illustrates the effect of varying the M_{OM}: M_{PG} on the UCS of OP-CLSM. As the proportion of OM increases, the UCS decreases significantly. For instance, OP-CLSM with OM0PG80 achieves a 7-day UCS of 0.52 MPa and a 28-day UCS of 1.77 MPa. In comparison, OP-CLSM containing OM80PG0 shows drastically reduced strength of 0.05 MPa (7d) and 0.12 MPa (28d) at $w_u = 20.65$ %, and just 0.01 MPa (7d) and 0.09 MPa (28d) at $w_u = 53.30$ %. Additionally, a higher proportion of OM not only diminishes absolute strength but also significantly slows the UCS strength development from 7 to 28 days. Qian et al. [97], Zhu et al. [53], and Do et al. [91] also reported that as the proportion of fine-grained soil in the fine aggregate increases, the strength of CLSM decreases markedly. The underlying mechanism is that high-packing-density aggregates (e.g., sand) are being replaced by fine-grained soil with lower packing density, resulting in an overall reduction in aggregate packing density. Consequently, this leads to increased porosity, a looser structure, and diminished UCS in CLSM [55]. Additionally, when the fine-grained soil is OM, its increased proportion will also raise the organic matter content of the aggregates. This inhibits both cement hydration and the subsequent pozzolanic reaction, both of which ultimately lead to a significant decrease in the UCS of OP-CLSM.

As depicted in Fig. 7(b), when the mix proportion of the fine aggregate (40 % OM + 40 % PG) and the binder dosage (12 % OPC + 8 % FA) are fixed, an increase in w_u of OM leads to a significant reduction in the 7 and 28-day UCS of OP-CLSM. For instance, as w_u increases from 14.41 % to 53.30 %, the 7-day UCS decreases from 0.26 MPa to 0.11 MPa, while the 28-day UCS decreases from 0.80 MPa to 0.32 MPa. This trend highlights the inhibitory effect of water-retentive OM on cement hydration and strength development.

Fig. 7(c) presents the relationship between a_{OPC}: a_{FA} and UCS. Increasing the proportion of cement OPC in the binders results in a near-linear growth trend in both 7-d and 28-d UCS, confirming the role of cement content in strength gain due to accelerated hydration and C-S-H gel formation. Fig. 7(d) evaluates the impact of different admixtures on UCS. It can be observed that in terms of enhancing the strength of OP-CLSM, PCE performs better than CaCl₂ and TEA. This is attributed to PCE's ability to improve particle dispersion and hydration efficiency, which fosters a denser microstructure.

An ideal CLSM should exhibit good fluidity, low bleeding rate, short setting time, and adequate strength. However, some of these properties are mutually conflicting, for example, high flowability often increases bleeding rate and reduces UCS. Therefore, CLSM design requires a careful balance to optimize these conflicting performance criteria [98]. Based on the experimental data and observed performance trends, it is recommended to produce OP-CLSM using fine aggregates composed of 30 %–40 % OM and 40 %–50 % PG (by dry material mass, totaling 80 %), combined with a binder consisting of 12 %–16 % OPC and 4 %–6 % FA (by dry material mass, totaling 20 %), and supplemented with 0.4 % PCE (by OPC mass). This composition offers a balanced solution that meets strength requirements while maintaining workability and environmental performance.

4.2.2. XRD and SEM

Fig. 8(a) presents the X-ray diffraction (XRD) patterns of five 28-day cured OP-CLSM specimens with a fixed organic matter content rate (w_u) of 53.30 %. The patterns display broad and noisy peaks between 20° and 40°, indicating a complex mineral composition of the soil sample. The primary mineral components identified include quartz (SiO₂), calcium sulfate (CaSO₄), and calcium carbonate (CaCO₃), which are the common constituents of both natural soil and industrial by-products. Additionally, hydration products such as
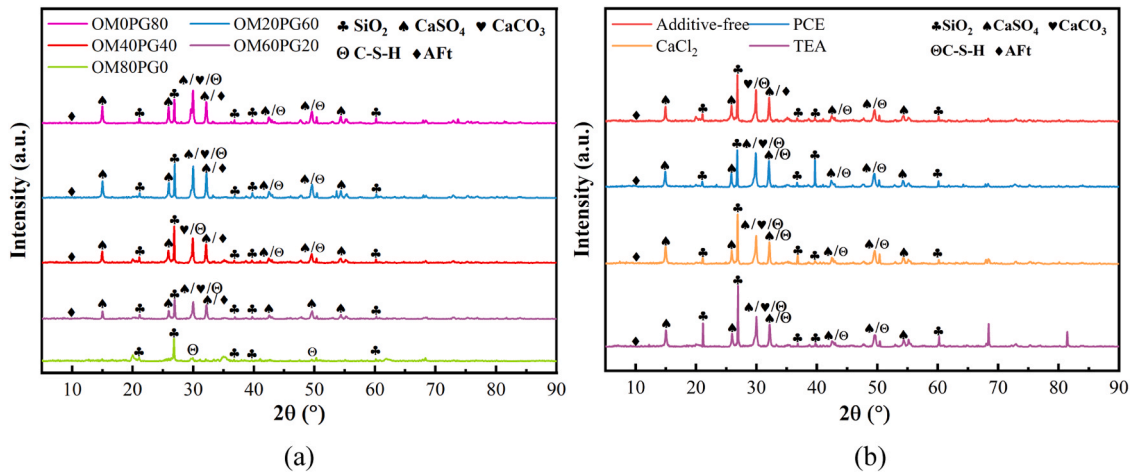

Fig. 8. XRD of OP-CLSM. (a) XRD of OP-CLSM after 28d curing (w_u=53.30 %); (b) XRD of OP-CLSM with different types of admixtures after 28d curing (w_u=53.30 %).

calcium silicate hydrate (C-S-H) and ettringite (AFt) are detected and typically formed from OPC and FA hydration reactions [74]. As the proportion of OM increases in the mixture, the intensity of diffraction peaks corresponding to C-S-H and AFt gradually diminishes. This trend implies that higher OM content reduces the formation of these critical hydration products. Notably, AFt is nearly undetectable in the XRD pattern of the OM80PG0 specimen, indicating that the formation of AFt primarily results from the hydration reactions associated with PG.

Fig. 8(b) shows the XRD patterns of OP-CLSM specimens cured for 28 days (w_u =53.30 %) with various admixtures. Within the 2θ range of 20° to 40°, the peak intensities associated with gelation products in specimens containing PCE and CaCl$_2$ are slightly higher than those in the control group without admixtures. In contrast, the peak intensity of the specimen containing TEA shows little deviation from that of the control OP-CLSM. This indicates that the PCE and CaCl$_2$ are more effective than TEA in promoting the generation of gelation products. These findings are consistent with the observed trends in the intensity enhancement law of OP-CLSM. Both PCE and CaCl$_2$ accelerate the cement hydration reaction through different mechanisms, thereby facilitating the formation of strength-contributing products such as C-S-H gel and AFt [45,111]. These products fill the pore structure, improve particle bonding, and enhance the overall mechanical performance of the OP-CLSM. Conversely, TEA exhibits a comparatively weaker effect on the formation of cementitious products, resulting in a less significant improvement in strength. The difference in XRD peak intensities further supports the superior 28-day compressive strength observed in OP-CLSM specimens incorporating PCE and CaCl$_2$.

The microstructural evolution of OP-CLSM is further illustrated in Fig. 9(a-h) through scanning electron microscopy (SEM). From Fig. 9(a) and (b), a dense matrix is observed where C-S-H gels and acicular-like AFt coat the surfaces of soil particles and fill interstitial voids, enhancing particle cohesion and forming a denser matrix. This well-structured network contributes to improved compressive strength. However, as the proportion of OM increases (accompanied by a reduction in PG), the amount of AFt significantly diminishes. SEM images in Fig. 9(c-e) reveal a looser and more porous microstructure, characterized by wider and more frequent voids between particles. This microstructural degradation aligns with the observed decline in both 7 and 28-day UCS values for high OM OP-CLSM mixtures. These microstructural observations confirm that OM not only physically dilutes the cementitious matrix but also chemically inhibits the formation of strength-contributing hydration products. The reduced production of C-S-H and AFt in high-OM mixes is a key factor behind the decline in mechanical performance.

Fig. 9(f-h) illustrates the microstructures of OP-CLSM specimens incorporating PCE, CaCl$_2$, and TEA, respectively. For comparison, Fig. 9(e) shows the microstructure of OP-CLSM without admixtures. The addition of PCE and CaCl$_2$ notably promotes the formation of C-S-H and AFt [71,99], resulting in a denser microstructure with fewer and smaller pores. This compact structure enhances interparticle bonding, thereby improving the mechanical strength of OP-CLSM. In contrast, although TEA also facilitates the formation of C-S-H and AFt (Fig. 9(h)), its effect is markedly weaker. Consequently, the microstructure remains relatively porous, with larger and more numerous voids compared to the specimens with PCE and CaCl$_2$. These observations are consistent with the trends identified in the XRD results.

4.3. Environmental safety of OP-CLSM

4.3.1. pH value

Previous studies have demonstrated that water-containing solid wastes exhibit corrosive properties when their pH falls below 2 or rises above 12.5 [100]. To evaluate the environmental safety of OP-CLSM, comprehensive testing and analysis of pH values are conducted across different curing ages and material compositions.

Fig. 10 presents the variation of pH values of OP-CLSM with curing time, considering conditions of differing fine aggregate ratios (M_{OM}: M_{PG}), organic matter contents (w_u), cement-fly ash mixing ratios (a_{OPC}: a_{FA}), and admixture types. Overall, the pH value decreases gradually with increasing curing time. This decline is primarily due to ongoing pozzolanic reactions that consume a significant amount of hydroxide ions (OH⁻) over time [101], consistent with the experimental patterns reported by Zeng et al. [74]. Analyzing Fig. 10 (a) and (b) reveals that increasing both the proportion of OM and w_u results in lower initial pH values. This is attributed to the presence of humic acid in the organic matter, which exhibits weak acidity [102]. Although OM reduces the pH value of OP-CLSM, all pH values across the tested specimens remain within the range of 10–12, indicating acceptable environmental safety levels. As shown in Fig. 10(c), the higher cement content (a_{OPC}) corresponds to increased pH values due to enhanced alkaline conditions from cement hydration. Meanwhile, Fig. 10(d) illustrates the variation in pH values of OP-CLSM over time with the addition of different admixtures (PCE, CaCl$_2$, and TEA), showing that specimens with admixtures consistently exhibit higher pH values than those without. The mechanisms behind this increase in pH due to admixtures are multifaceted: 1) Some admixtures, such as PCE and TEA, are weakly alkaline in nature; 2) They promote cement hydration, which leads to the production and dissolution of Ca(OH)$_2$, thereby increasing hydroxide ion (OH⁻) concentration in the pore solution [99,103,104].

4.3.2. Leachability of harmful substances

The concentrations of potentially harmful substances identified in the untreated PG and two OP-CLSM specimens cured for 28 days are summarized in Table 6. The raw PG material exhibited levels of arsenic (As, 0.126 mg/L), phosphorus (P, 120.00 mg/L), and fluorine (F, 105.00 mg/L) that substantially exceed the permissible limits for Class IV water quality, which is suitable for some industrial applications and agricultural use [105]. In contrast, these elements are significantly attenuated in the OP-CLSM samples, with all measured concentrations falling below the regulatory thresholds for Class IV water [105]. This key result directly verifies that the CLSM matrix effectively immobilizes hazardous substances in PG, confirming the environmental feasibility of using PG as a fine aggregate in OP-CLSM.

This reduction is attributed to several mechanisms initiated during the solidification process, including: 1) Micro-scale physical
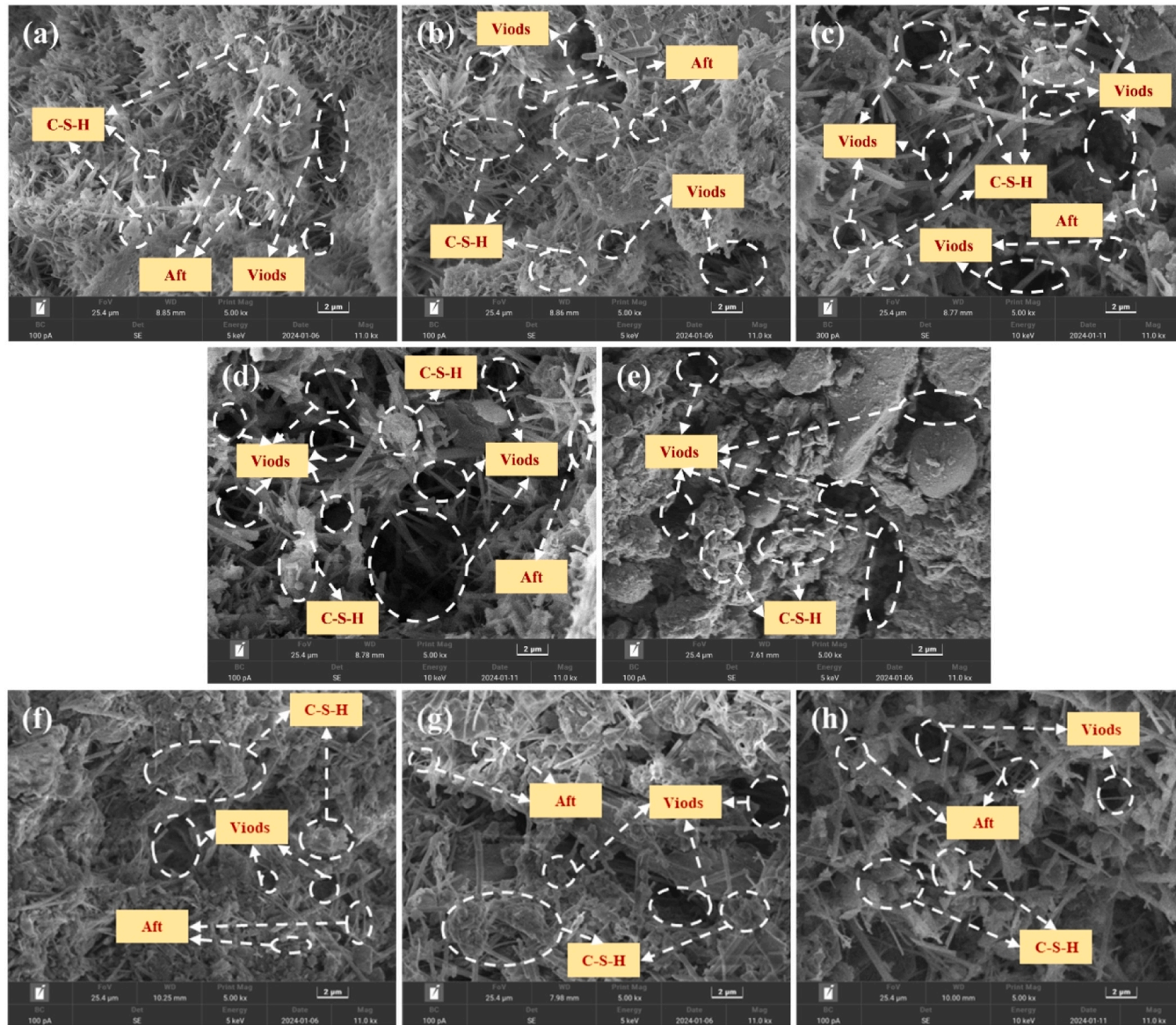
Fig. 9. SEM images of OP-CLSM after 28d curing (w_u=53.30 %). (a) OM0PG80; (b) OM20PG60; (c) OM40PG40; (d) OM60PG20; (e) OM80PG0; (f) Add PCE; (g) Add CaCl$_2$; (h) Add TEA.
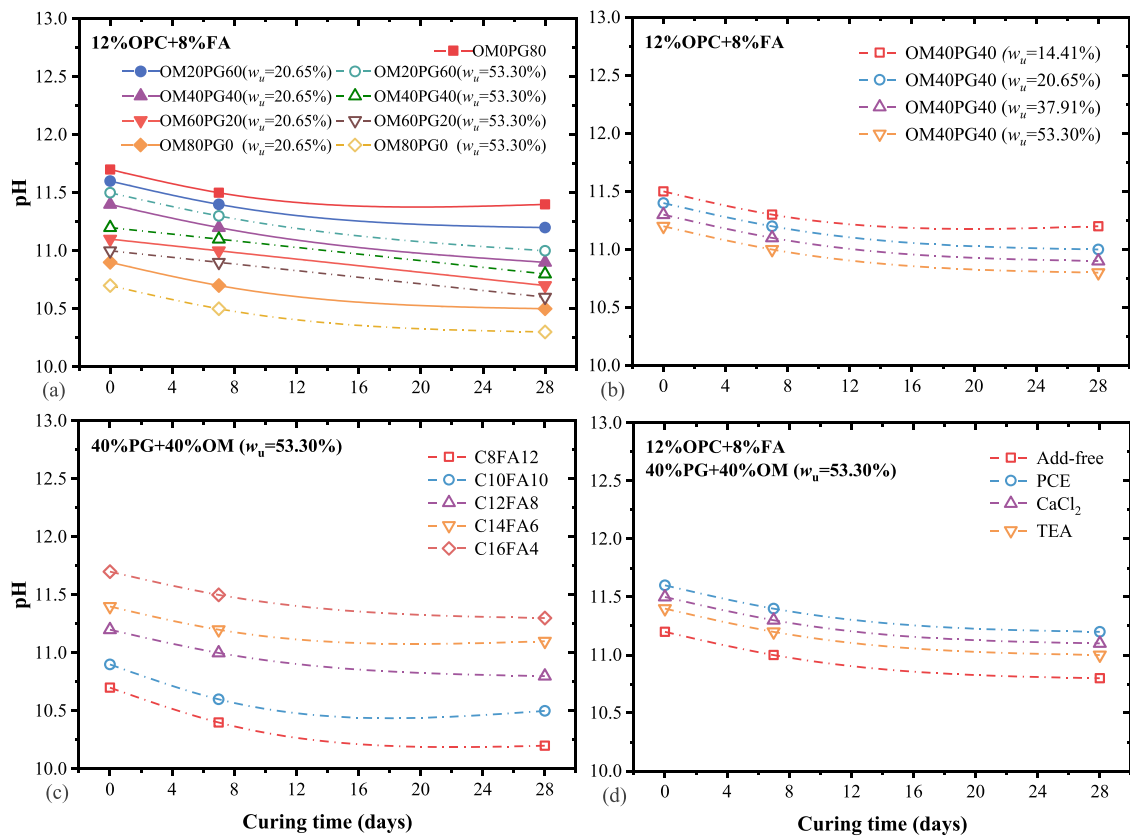
Fig. 10. pH of OP-CLSM under different effect indexes. (a) M_{OM}: M_{PG}; (b) w_u; (c) a_{OPC}: a_{FA}; (d) Types of admixtures.

Table 6
Elemental concentrations of leachates in the acid leaching test (mg/L).

Sample	As	Cd	Ba	Pb	Zn	P	F
PG	0.1263	< 0.020	0.0699	< 0.020	1.4146	120.00	105.00
OM40PG40 (w_u=53.30 %)	0.0264	< 0.0012	0.333	< 0.0042	< 0.0064	0.0733	1.790
OM40PG40 (w_u=20.65 %)	0.0462	< 0.0012	0.285	< 0.0042	< 0.0064	0.103	1.780
GB/T 14848: Category IV	0.050	0.010	4.000	0.100	5.000	/	2.000

Note: "P" refers to phosphide; "F" refers to fluoride; GB/T 14848: Category IV [105].

confinement and sorption within hydration products, such as C-S-H and AFt, which effectively entrap contaminants and limit their leachability [106]; 2) Precipitation chemical reactions under the highly alkaline conditions of OP-CLSM, where metal ions and fluoride (F^-) form poorly soluble compounds, such as calcium fluoride (CaF_2), via reactions like $Ca^{2+} + 2 F^- \rightarrow CaF_2\downarrow$ [107]; 3) Isomorphic substitution of Ca^{2+} by heavy metals within the crystalline structures of hydration phases, including C-S-H, calcium aluminate hydrate (C-A-H), and AFt, thereby creating chemically stable matrices resistant to leaching [108]; 4) Electrostatic adsorption onto cementitious and soil particles, whose extensive surface areas enable the capture of anionic species like phosphate (PO_4^{3-}) through ion exchange and surface complexation processes [109,110].

5. Overall summary of application, synergistic, economical and sustainable benefits of OP-CLSM

The above test analysis indicates that OP-CLSM meets the standards for typical workability, 28-day strength, and key environmental safety requirements. Similar to conventional CLSM, its main engineering applications,such as foundation pit fat groove backfilling, retaining wall backfilling, low-grade construction access road embankment filling, and trench backfilling, effectively support the growing demand for urban renewal. Ultimately, this approach promotes the large-scale utilization and comprehensive management of the two major types of solid waste in Kunming.

By applying the principle of "waste treating waste", OP-CLSM incorporates OM and PG as its primary constituents, with their combined proportion reaching up to 80 % of the total dry material content. This approach not only facilitates the recycling of two major solid waste streams but also significantly reduces the volume of OM requiring off-site disposal, thereby lowering associated

transportation and treatment costs. Additionally, it promotes the large-scale resource utilization of stockpiled PG, addressing two long-standing challenges in urban development in Kunming: the disposal of OM and the environmental burden posed by accumulated PG.

The combination of OM and PG as composite fine aggregates in OP-CLSM produces a synergistic effect, optimizing the material engineering performance. When OM is used as the sole fine aggregate (OM80PG0), the resulting CLSM exhibits low UCS, ranging from 0.01 to 0.05 MPa at 7 days and 0.09–0.12 MPa at 28 days, along with prolonged initial and final setting times exceeding 24 h. Conversely, using PG as the sole fine aggregate (OM0PG80) results in a high bleeding rate of 14.41 %, compromising stability. However, the excellent water retention capacity of OM effectively reduces the bleeding rate of OP-CLSM, while PG contributes to enhanced compactness, strength, and stiffness. These complementary properties create a synergistic interaction between OM and PG, significantly improving the overall engineering performance and ensuring the environmental safety of OP-CLSM in compliance with relevant standards.

OP-CLSM offers a cost-effective solution with strong potential for large-scale applications. For example, preparing 1 m³ of OP-CLSM (ID: OM40PG40, Binder: 12 % OPC + 8 % FA) requires approximately 118 kg of OPC and 59 kg of FA. Since the fine aggregate consists of two types of solid wastes (OM and PG), incurring no material cost. Additionally, the transportation of PG from the tailings pond west of Dianchi Lake to Kunming's northeastern main urban area covers a manageable distance of 40–80 km, resulting in reasonable transport expenses. Therefore, the total material cost, including binders, admixtures, tap water, and PG transportation, is approximately 78–84 RMB/m³ . The total carbon emissions from OP-CLSM production, accounting for raw materials production and the PG transportation, are approximately 99.8 kg/m³ . Overall, OP-CLSM demonstrates lower costs and carbon emissions compared to typical CLSM (cost: 135.2–339.3 RMB/m³; carbon emissions: 139–182 kg/m³) [90]. Collectively, these factors enhance the economic viability and scalability of OP-CLSM for urban construction and sustainable waste management.

6. Conclusion

This study systematically evaluated the feasibility of using a mixture of OM and PG as fine aggregates in the preparation of OP-CLSM, aiming to promote the large-scale reuse of industrial and construction waste materials. A series of laboratory experiments were conducted to investigate the effects of various mix proportions, organic matter content, binder ratios, and chemical admixtures on the fresh and hardened properties of OP-CLSM. The key conclusions are as follows:

1) With appropriate mix designs, the optimized OP-CLSM incorporating OM and PG as composite fine aggregates achieved desirable engineering properties, including high flowability (>150 mm), acceptable bleeding rates (0.7 – 7.0 %), short setting times (<24 h), moderate unconfined compressive strength (0.3–1.8 MPa), and satisfactory environmental safety that is characterized by an alkaline pH (10−12) and leaching concentrations of harmful substances compliant with the limits specified in GB/T 14848: Category IV.
2) Due to the water retention capacity of organic matter and its inhibitory effect on cement hydration, increasing either the OM proportion or the w_u in OM significantly reduces the fluidity, bleeding rate, and unconfined compressive strength (UCS) of OP-CLSM, while also prolonging the setting time.
3) Among the tested admixtures, polycarboxylate superplasticizer (PCE) exhibited superior performance in enhancing fluidity, reducing bleeding and setting time, and increasing compressive strength, outperforming both calcium chloride (CaCl₂) and triethanolamine (TEA).
4) Suitable performance of OP-CLSM is achieved with fine aggregates composed of 30 % - 40 % OM and 40 % - 50 % PG (dry material mass ratio, totaling 80 %), combined with 12 % - 16 % Ordinary Portland cement (OPC) and 4 % - 6 % fly ash (FA) (dry material mass ratio, totaling 20 %) as stabilizers, and 0.4 % PCE (by OPC mass).

CRediT authorship contribution statement

Declaration of Competing Interest

Acknowledgements

Technology. The authors also gratefully acknowledge the financial support from the National Natural Science Foundation of China (Grant Nos. 52068039, 52468052, and 52408367). Additionally, the authors also sincerely appreciate the support of Yunnan Yuntianhua Co., Ltd. in supplying the phosphogypsum used in this study.

Data availability

Data will be made available on request.

References

[1] B.B. Huat, S. Kazemian, A. Prasad, M. Barghchi, State of an art review of peat: General perspective, Int. J. Phys. Sci. 6 (8) (2011) 1988–1996.

[2] G. Mesri, M. Ajlouni, Engineering properties of fibrous peats, Geotech. Geoenviron. Eng 133 (7) (2007) 850–866.

[3] Y. Gui, Z.H. Yu, H.M. Liu, J. Cao, Z.C. Wang, Secondary consolidation properties and mechanism of plateau lacustrine peaty soil, Chin. J. Geotech. Eng 37 (8) (2015) 1390–1398.

[4] P. van Elderen, G. Erkens, C. Zwanenburg, H. Middelkoop, E. Stouthamer, Viscous compression of clay and peat, Earth Sci. Rev. (2024) 104993.

[5] GB 50202-18, 2018. Standard for Acceptance of Construction Quality of Building Foundation. Ministry of Housing and Urban-Rural Development of the People's Republic of China, Beijing, China.

[6] M. Liu, M. Saberian, J. Li, J. Zhu, S.T.A.M. Perera, R. Roychand, A. Tajaddini, Evaluation of brown coal fly ash for stabilising expansive clay subgrade: A sustainable solution for pavement construction, Resour. Conserv. Recycl 204 (2024) 107533.

[7] W. Hassan, A.S.A. Rashid, N. Latifi, S. Horpibulsuk, S. Borhamdin, Strength and morphological characteristics of organic soil stabilized with magnesium chloride, Q. J. Eng. Geol. Hydrogeol 50 (4) (2017) 454–459.

[8] L.S. Wong, R. Hashim, F. Ali, Utilization of sodium bentonite to maximize the filler and pozzolanic effects of stabilized peat, Eng. Geol 152 (1) (2013) 56–66.

[9] S. Wang, X. He, S. Gong, G. Cai, L. Lang, H. Ma, Z. Niu, F. Zhou, Influence mechanism of fulvic acid on the strength of cement-solidified dredged sludge, Water 14 (17) (2022) 2616.

[10] C. Du, J. Zhang, G. Yang, Q. Yang, The influence of organic matter on the strength development of cement-stabilized marine soft clay. Mar. Georesources Geotechnol 39 (8) (2021) 983–993.

[11] H. Beddaa, A.B. Fraj, F. Lavergne, J.M. Torrenti, Effect of potassium humate as humic substances from river sediments on the rheology, the hydration and the strength development of a cement paste, Cem. Concr. Compos 104 (2019) 103400.

[12] M.E. Jorat, S. Kreiter, T. Mörz, V. Moon, W. de Lange, Strength and compressibility characteristics of peat stabilized with sand columns, Geomech. Engg 5 (6) (2013) 575–594.

[13] B. Kalantari, R.K. Rezazade, Compressibility behaviour of peat reinforced with precast stabilized peat columns and FEM analysis, Geomech. Eng. 9 (4) (2015) 415–426.

[14] G. Mesri, M. Ajlouni, Engineering properties of fibrous peats. Geotech, Geoenviron. Eng. 133 (7) (2007) 850–866.

[15] A. Ahmad, M.H. Sutanto, M.A.M. Al-Bared, I.S.H. Harahap, S.V.A.N.K. Abad, M.A. Khan, Physio-chemical properties, consolidation, and stabilization of tropical peat soil using traditional soil additives—A state of the art literature review, KSCE J. Civ. Eng. 25 (10) (2021) 3662–3678.

[16] S. Ghadr, A. Assadi Langroudi, C. Hung, Stabilisation of peat with colloidal nanosilica, Mires and Peat, 26(Art. 9) (2020).

[17] B. Pokharel, S. Siddiqua, Effect of calcium bentonite clay and fly ash on the stabilization of organic soil from Alberta, Can, Eng. Geol 293 (2021) 106291.

[18] A. Ahmad, M.H. Sutanto, N.R.B. Ahmad, M. Bujang, M.E. Mohamad, The implementation of industrial byproduct in malaysian peat improvement: A sustainable soil stabilization approach, Materials 14 (23) (2021) 7315.

[19] S.A. Mazlan, D.Z.A. Hasbollah, M.K.A. Legiman, A.M. Taib, A. Ibrahim, A.B. Ramli, S.N. Jusoh, N.A. Rahman, M.F.M. Dan, A. Zukri, Effectiveness of coffee husk ash and coconut fiber in improving peat properties, Phys. Chem. Earth, Parts A/B/C 130 (2023) 103361.

[20] M. Saberian, M.A. Rahgozar, Geotechnical properties of peat soil stabilised with shredded waste tyre chips in combination with gypsum, lime or cement, Mires and Peat 18 (2016) 16.

[21] J. Wang, M. Li, Z. Wang, L. Shen, The benefits of using manufactured sand with cement for peat stabilisation: An experimental investigation of physico-chemical and mechanical properties of stabilised peat, Bull. Eng. Geol. Environ 79 (2020) 4441–4460.

[22] Y. Chernysh, O. Yakhnenko, V. Chubur, H. Roubík, Phosphogypsum recycling: a review of environmental issues, current trends, and prospects, Appl. Sci. 11 (4) (2021) 1575.

[23] B. Cichy, H. Jaroszek, Phosphogypsum management. World and Polish practice, Przemysl Chemiczny 92 (7) (2013) 1336–1340.

[24] E. Bilal, H. Bellefqih, V. Bourgier, H. Mazouz, D.G. Dumitraş, F. Bard, M. Laborde, J.P. Caspar, B. Guilhot, E.L. Iatan, M. Bounakhla, Phosphogypsum circular economy considerations: A critical review from more than 65 storage sites worldwide, J. Clean. Prod 414 (2023) 137561.

[25] K. Grabas, A. Pawełczyk, W. Stręk, E. Szełęg, S. Stręk, Study on the properties of waste apatite phosphogypsum as a raw material of prospective applications, Waste Biomass Valori 10 (2019) 3143–3155.

[26] H. Tayibi, M. Choura, F.A. López, F.J. Alguacil, A. López-Delgado, Environmental impact and management of phosphogypsum, J. Environ. Manag 90 (8) (2009) 2377–2386.

[27] J. Men, Y. Li, P. Cheng, Z. Zhang, Recycling phosphogypsum in road construction materials and associated environmental considerations: A review, Heliyon 8 (2022) 11.

[28] S. Meskini, A. Samdi, H. Ejjaouani, T. Remmal, Valorization of phosphogypsum as a road material: Stabilizing effect of fly ash and lime additives on strength and durability, J. Clean. Prod 323 (2021) 129161.

[29] Y. Thakur, A. Tyagi, S. Sarkar, Utilization of industrial waste phosphogypsum as geomaterial: a review, J. Hazard. Tox. Radioact. Waste 27 (2) (2023) 03123001.

[30] C.Q. Wang, S. Chen, D.M. Huang, Q.C. Huang, X.Q. Li, Z.H. Shui, Safe environmentally friendly reuse of red mud modified phosphogypsum composite cementitious material, Constr. Build. Mater 368 (2023) 130348.

[31] H. Yue, A. Fang, S. Hua, Z. Gu, J. Yu, Y. Cheng, Development and field application of phosphogypsum-based soil subgrade stabilizers, J. Renew. Mater 10 (8) (2022) 2247.

[32] G. Luan, F. Zhao, J. Xia, Z. Huang, S. Feng, C. Song, P. Dong, X. Zhou, Analysis of long-term spatio-temporal changes of plateau urban wetland reveals the response mechanisms of climate and human activities: A case study from Dianchi Lake Basin 1993–2020, Sci. Total Environ 912 (2024) 169447.

[33] Q. Chen, Q. Zhang, A. Fourie, C. Xin, Utilization of phosphogypsum and phosphate tailings for cemented paste backfill, J. Environ. Manag 201 (2017) 19–27.

[34] Keyao, C., 2024. Kunming has comprehensively promoted the comprehensive utilization of phosphogypsum, with the comprehensive utilization rate exceeding 70% in 2023. ⟨http://res.cenews.com.cn/hjw/news.html?aid=1109217⟩.

[35] Y. Gui, L. Pu, S. Lu, M. Xie, L. Pei, Y. Tian, Physical, mechanical, compaction, and leaching properties of phosphogypsum-based semi-rigid aggregated geomaterial, J. Clean. Prod (2025) 145664.

[36] ACI 229R-13, Report on controlled low-strength materials, American Concrete Institute (ACI), Farmington Hills, MI, USA, 2013.

[37] T. Chompoorat, S. Likitlersuang, P. Jongvivatsakul, The performance of controlled low-strength material base supporting a high-volume asphalt pavement, KSCE J. Civ. Eng. 22 (6) (2018) 2055–2063.

[38] W. Han, D. Lee, J.-S. Lee, D.S. Lim, H.-K. Yoon, Prediction of flowability and strength in controlled low-strength material through regression and oversampling algorithm with deep neural network, Case Stud. Constr. Mater 20 (2024) e03192.

[39] D.G. Son, J.-S. Lee, S. Kim, Y.-H. Byun, Permanent strain behavior of basalt fiber–reinforced controlled low-strength material under repeated loading, Transp. Geotech 52 (2025) 101570.

[40] T. Chompoorat, N. Sangsai, W. Tanapalungkorn, P. Chindasiriphan, P. Nuaklong, P. Jongvivatsakul, S. Likitlersuang, Cement-based and alkali-activated controlled low-strength materials made from cup lump rubber for use as road materials, Road Mater. Pavement Des 26 (6) (2025) 1151–1171.

[41] Y.G. Heo, D.G. Son, Q.O. Babatunde, Y.-H. Byun, Controlled low strength material modified with lignosulfonate, Int. J. Geo-Eng 15 (2024) 1–12.

[42] P. Chindasiriphan, C. Punyasuth, K. Hamcumpai, N. Kongmalai, P. Jongvivatsakul, T. Chompoorat, W. Tanapalungkorn, S. Likitlersuang, Repurposing plastic bottle cap waste in controlled low-strength material for pavement base applications, Clean. Mater 17 (2025) 100335.

[43] M. Lachemi, K.M. Hossain, M. Shehata, W. Thaha, Characteristics of controlled low-strength materials incorporating cement kiln dust, Can. J. Civ. Eng 34 (4) (2007) 485–495.

[44] M. Lachemi, M. Şahmaran, K.M.A. Hossain, A. Lotfy, M. Shehata, Properties of controlled low-strength materials incorporating cement kiln dust and slag, Cem. Concr. Compos 32 (8) (2010) 623–629.

[45] H.Y. Wang, K.W. Chen, A study of the engineering properties of CLSM with a new type of slag, Constr. Build. Mater 102 (2016) 422–427.

[46] T. Chompoorat, T. Thepumong, P. Nuaklong, P. Jongvivatsakul, S. Likitlersuang, Alkali-activated controlled low-strength material utilizing high-calcium fly ash and steel slag for use as pavement materials, J. Mater. Civ. Eng 33 (8) (2021) 04021152.

[47] M. Mahamaya, S.K. Das, Characterization of ferrochrome slag as a controlled low-strength structural fill material, Int. J. Geotech. Eng 14 (3) (2018) 312–321.

[48] M. Mahamaya, S. Jain, S.K. Das, R. Paul, Engineering properties of cementless alkali-activated CLSM, using ferrochrome slag. J. Mater. Civ. Eng 35 (8) (2023) 04023177.

[49] S. Naganathan, H.A. Razak, S.N.A. Hamid, Properties of controlled low-strength material made using industrial waste incineration bottom ash and quarry dust, Materials & Design 33 (2012) 56–63.

[50] T.M. Do, H.K. Kim, M.J. Kim, Y.S. Kim, Utilization of controlled low strength material (CLSM) as a novel grout for geothermal systems: Laboratory and field experiments, J. Build. Eng 29 (2020) 101110.

[51] D.Y. Yan, I.Y. Tang, I.M. Lo, Development of controlled low-strength material derived from beneficial reuse of bottom ash and sediment for green construction, Constr. Build. Mater 64 (2014) 201–207.

[52] J. Du, L. Zhang, Q. Hu, Q. Luo, D.P. Connolly, K. Liu, T. Hu, J. Zhu, T. Wang, Characterization of controlled low-strength materials from waste expansive soils, Constr. Build. Mater 411 (2024) 134690.

[53] Y. Zhu, D. Liu, G. Fang, H. Wang, D. Cheng, Utilization of excavated loess and gravel soil in controlled low strength material: Laboratory and field tests, Constr. Build. Mater 360 (2022) 129604.

[54] X. Sun, W. Liu, X. Chen, S. Wu, G. Chen, Y. Bi, Z. Chen, Sustainable solutions: Transforming waste shield tunnelling soil into geopolymer-based underwater backfills, J. Clean. Prod 445 (2024) 141363.

[55] G. Zhao, X. Pan, H. Yan, J. Tian, Y. Han, B. Liu, S. Wang, Utilization of high fine-grained shield tunnel spoil in CLSM and effect of foam agent content on properties, Constr. Build. Mater 423 (2024) 135836.

[56] J. Zhang, J. Wang, X. Li, T. Zhou, Y. Guo, Rapid-hardening controlled low strength materials made of recycled fine aggregate from construction and demolition waste, Constr. Build. Mater 173 (2018) 81–89.

[57] S.K. Das, M. Mahamaya, K.R. Reddy, Coal mine overburden soft shale as a controlled low strength material, Int. J. Min. Reclam. Environ 34 (8) (2020) 543–557.

[58] M. Mahamaya, S. Alam, S.K. Das, Development and characterization of alkali-activated controlled low-strength material using mining waste, Constr. Build. Mater 452 (2024) 138928.

[59] D.A. Ghanad, A. Soliman, S. Godbout, J. Palacios, Properties of bio-based controlled low strength materials, Constr. Build. Mater 262 (2020) 120742.

[60] J.Y. Wu, M. Tsai, Feasibility study of a soil-based rubberized CLSM, Waste Manag 29 (2) (2009) 636–642.

[61] S. Naganathan, H.A. Razak, S.N.A. Hamid, Effect of kaolin addition on the performance of controlled low-strength material using industrial waste incineration bottom ash, Waste Manag. Res. 28 (9) (2010) 848–860.

[62] B.J. Kim, J.G. Jang, C.Y. Park, O.H. Han, H.K. Kim, Recycling of arsenic-rich mine tailings in controlled low-strength materials, J. Clean. Prod 118 (2016) 151–161.

[63] L. Wang, W. Feng, S.A.M. Lazaro, X. Li, Y. Cheng, Z. Wang, Engineering properties of soil-based controlled low-strength materials made from local red mud and silty soil, Constr. Build. Mater 358 (2022) 129453.

[64] S. Zhang, N. Jiao, J. Ding, C. Guo, P. Gao, X. Wei, Utilization of waste marine dredged clay in preparing controlled low strength materials with polycarboxylate superplasticizer and ground granulated blast furnace slag, J. Build. Eng 76 (2023) 107351.

[65] Y. Wu, J. Geng, H. Zhu, C. Jin, N. Kang, Development and Characterization of Sustainable Cement-Free Controlled Low Strength Material Using Titanium Gypsum and Construction Waste Soil, Materials 17 (23) (2024) 5698.

[66] H.Z. Zhu, F.Q. Yu, J. Geng, Strength and volume stability of controlled low-strength material based on titanium gypsum. Bull, Chin. Ceram. Soc. 40 (11) (2021) 3644–3653.

[67] L. Wang, J.S. Kwok, D.C. Tsang, C.S. Poon, Mixture design and treatment methods for recycling contaminated sediment, J. Hazard. Mater 283 (2015) 623–632.

[68] H.A. Razak, S. Naganathan, S.N.A. Hamid, Performance appraisal of industrial waste incineration bottom ash as controlled low-strength material, J. Hazard. Mater 172 (2-3) (2009) 862–867.

[69] C. Wang, Y. Li, P. Wen, W. Zeng, X. Wang, A comprehensive review on mechanical properties of green controlled low strength materials, Constr. Build. Mater 363 (2023) 129611.

[70] A.J. Puppala, B. Chittoori, A. Raavi, Flowability and density characteristics of controlled low-strength material using native high-plasticity clay, J. Mater. Civil Eng 27 (1) (2015) 06014026.

[71] L. Wang, F. Zou, X. Fang, D.C. Tsang, C.S. Poon, Z. Leng, K. Baek, A novel type of controlled low strength material derived from alum sludge and green materials, Constr. Build. Mater 165 (2018) 792–800.

[72] T. Chompoorat, P. Jongpradist, C.D. Dejdonbomand, Utilization of para rubber latex and geopolymer-stabilized laterite as bases and subbases, J. Mater. Civ. Eng 37 (2) (2025) 04025001.

[73] A. Dixit, S. Jain, S.K. Das, A systematic characterization of the mixture of red mud and bottom ash as a geomaterial: an efficient utilization in subgrade pavement, J. Mater. Cycles Waste Manag 26 (4) (2024) 2159–2174.

[74] L.L. Zeng, X. Bian, L. Zhao, Y.J. Wang, Z.S. Hong, Effect of phosphogypsum on physiochemical and mechanical behaviour of cement stabilized dredged soil from Fuzhou, China. Geomech, Energy Environ 25 (2021) 100195.

[75] L. Zeng, X. Bian, J. Weng, T. Zhang, Wetting-drying effect on the strength and microstructure of cement-phosphogypsum stabilized soils, J. Rock Mech. Geotech. Eng 16 (3) (2024) 1049–1058.

[76] ASTM D2216-19, Standard Test Methods for Laboratory Determination of Water (Moisture) Content of Soil and Rock by Mass, American Society for Testing and Materials, West Conshohocken, PA, US, 2019.

[77] ASTM D2974-20, Standard Test Methods for Determining the Water (Moisture) Content, Ash Content, and Organic Material of Peat and Other Organic Soils, American Society for Testing and Materials, West Conshohocken, PA, US, 2020.

[78] GB/T 50123-19, Standard for geotechnical testing method, China Planning Press, Beijing, China, 2019.

[79] ASTM D7348-21, Standard test methods for loss on ignition (LOI) of solid combustion residues, American Society for Testing and Materials, West Conshohocken, PA, US, 2021.

[80] ASTM D1997-20, Standard test method for laboratory determination of the fiber content of peat, American Society for Testing and Materials, West Conshohocken, PA, US, 2020.

[81] ASTM D4427-18, Standard classification of peat samples by laboratory testing, American Society for Testing and Materials, West Conshohocken, PA, US, 2018.

[82] ASTM D6103M-17, Standard test method for flow consistency of controlled low strength material (CLSM), American Society for Testing and Materials, West Conshohocken, PA, US, 2017.

[83] ASTM C940-22, Standard test method for expansion and bleeding of freshly mixed grouts for preplaced-aggregate concrete in the laboratory, American Society for Testing and Materials, West Conshohocken, PA, USA, 2022.

[84] GB/T 1346-11, Test methods for water requirement of normal consistency, setting time and soundness of the Portland cement, China Standards Press, Beijing, China, 2011.

[85] ASTM C191-21, Standard Test Methods for Time of Setting of Hydraulic Cement by Vicat Needle, American Society for Testing and Materials, West Conshohocken, PA, US, 2021.

[86] ASTM D2166/D2166M-24, Standard test method for unconfined compressive strength of cohesive soil, American Society for Testing and Materials, West Conshohocken, PA, US, 2024.

[87] ASTM D4972-19, Standard test methods for pH of soils, American Society for Testing and Materials, West Conshohocken, PA, US, 2019.

[88] EPA Method 1311, Toxicity characteristic leaching procedure, U.S. Environmental Protection Agency, Washington, D.C., US, 1992.

[89] T. Chen, N. Yuan, S. Wang, X. Zhang, C. Lin, X. Wu, Q. Wang, D. Wang, Optimization of controlled low-strength material from multi-component coal-based solid waste, Sustainability 16 (2024) 1513.

[90] T. Zhang, Y. Jianming, W. Wang, P. Chen, C. Chen, Z. Wu, J. Wei, Q. Yu, Efficient utilization of waste shield slurry and CDW, fines to prepare eco-friendly controlled low-strength material. J. Clean. Prod 444 (2024) 141343.

[91] T.M. Do, A.N. Do, O.K. Gyeong, Y.S. Kim, Utilization of marine dredged soil in controlled low-strength material used as a thermal grout in geothermal systems, Constr. Build. Mater 215 (2019) 613–622.

[92] U. Salini, A. Parayil, B. Diya, L. Dev, Use of fly ash and quarry waste for the production of the controlled low strength material, Constr. Build. Mater 392 (2023) 131924.

[93] P. Chindasiriphan, H. Yokota, P. Pimpakan, Effect of fly ash and superabsorbent polymer on concrete self-healing ability, Constr. Build. Mater 233 (2020) 116975.

[94] N.K. Lee, H.K. Kim, I.S. Park, H.K. Lee, Alkali-activated, cementless, controlled low-strength materials (CLSM) utilizing industrial by-products, Constr. Build. Mater 49 (2013) 738–746.

[95] S.K. Kaliyavaradhan, T.C. Ling, M.Z. Guo, K.H. Mo, Waste resources recycling in controlled low-strength material (CLSM): A critical review on plastic properties, J. Environ. Manag 241 (2019) 383–396.

[96] S.D. Khadka, O. Okuyucu, P.W. Jayawickrama, S. Senadheera, Controlled low strength materials (CLSM) activated with alkaline solution: Flowability, setting time and microstructural characteristics, Case Stud. Constr. Mater 18 (2023) e01892.

[97] J. Qian, Y. Hu, J. Zhang, W. Xiao, J. Ling, Evaluation the performance of controlled low strength material made of excess excavated soil, J. Clean. Prod 214 (2019) 79–88.

[98] S.K. Parhi, S. Dwibedy, S. Panda, S.K. Panigrahi, A comprehensive study on controlled low strength material, J. Build. Eng 76 (2023) 107086.

[99] J. Zhu, J. Hui, H. Luo, B. Zhang, X. Wei, F. Wang, Y. Li, Effects of polycarboxylate superplasticizer on rheological properties and early hydration of natural hydraulic lime, Cem. Concr. Compos 122 (2021) 104052.

[100] Tikalsky, P.J., Bahia, H.U., Deng, A. and Snyder, T., 2004. Tikalsky, P.J., Bahia, H.U., Deng, A. and Snyder, T., 2004. Excess foundry sand characterization and experimental investigation in controlled low-strength material and hot-mixing asphalt. The Pennsylvania transportation Institute, The Pennsylvania State University, PA, United States.

[101] K. Scrivener, A. Ouzia, P. Juilland, A.K. Mohamed, Advances in understanding cement hydration mechanisms, Cem. Concr. Compos 124 (2019) 105823.

[102] Z. Wang, M. Li, L. Shen, J. Wang, Incorporating clay as a natural and enviro-friendly partial replacement for cement to reduce carbon emissions in peat stabilisation: An experimental investigation, Constr. Build. Mater 353 (2022) 128901.

[103] J. Han, K. Wang, J. Shi, Y. Wang, Influence of sodium aluminate on cement hydration and concrete properties, Constr. Build. Mater 64 (2014) 342–349.

[104] Y.L. Yaphary, Z. Yu, R.H. Lam, D. Lau, Effect of triethanolamine on cement hydration toward initial setting time, Constr. Build. Mater 141 (2017) 94–103.

[105] GB/T 14848-17, Standard for groundwater quality, China Standards Press, Beijing, China, 2017.

[106] Y. Yao, X. Wang, B.L. Yan, L. Wang, C. Liu, The research on heavy metal ions curing and its influence on the cement hydration process. Bull. Chin. Ceram. Soc. 31 (5) (2012) 1138–1144.

[107] A. Lewis, Precipitation of heavy metals. In Sustainable Heavy Metal Remediation: Volume 1: Principles and Processes, Springer International Publishing, Cham, 2017, pp. 101–120.

[108] T. Deng, H. Liu, J. Ni, H. Ke, L. Li, Y. Deng, Pb2+ Leachability in the Cement-Based Solidified/Stabilized Contaminated Clay Under Saline and Alkaline Environments. Soil Sediment Contam, Int. J. 34 (2) (2025) 276–290.

[109] A. Ioannou, A. Dimirkou, Phosphate adsorption on hematite, kaolinite, and kaolinite–hematite (k–h) systems as described by a constant capacitance model, J. Colloid Interface Sci 192 (1) (1997) 119–128.

[110] A.D. Karathanasis, P.D. Shumaker, Organic and inorganic phosphate interactions with soil hydroxy-interlayered minerals, J. Soils Sediments 9 (2009) 501–510.

[111] L. Wang, S.S. Chen, D.C.W. Tsang, C.S. Poon, K. Shih, Value-added recycling of construction waste wood into noise and thermal insulating cement-bonded particleboards, Constr. Build. Mater 125 (2016) 316–325.